Science & Technology Facilities Council

Technical Report
RAL-TR-2017-005

# The feasibility of integrating supercapacitor energy storage in wind turbines

AJ Ruddell

April 2017

Enquiries concerning this report should be addressed to:

RAL Library
STFC Rutherford Appleton Laboratory
Harwell Oxford
Didcot
OX11 0QX

Tel: +44(0)1235 445384
Fax: +44(0)1235 446403
email: libraryral@stfc.ac.uk

Science and Technology Facilities Council reports are available online at: http://epubs.stfc.ac.uk

**ISSN 1358-6254**

# The feasibility of integrating supercapacitor energy storage in wind turbines

A J Ruddell

Energy Research Unit
STFC Rutherford Appleton Laboratory

April 2017

## Summary

The aim of the work is to investigate the feasibility of using supercapacitor energy storage in wind turbines, and to conduct a cost-benefit analysis. The report draws on information presented in a Supergen Wind Energy Technologies (Phase 2) deliverable report.

Consideration of the Grid code requirement for fault ride through (FRT) in response to voltage dips resulted in an estimated energy storage capacity equivalent to rated power for up to one second.

A Supercapacitor Energy Storage System (SCESS) using a stack of supercapacitor modules was specified and the equivalent circuit parameters were provided for inclusion in a simulation model. The gravimetric and volumetric densities for the SCESS were estimated. Inertial storage in a wind turbine rotor was also specified using a relationship for the inertia trend with wind turbine size, derived in Appendix D of this report.

Experiments were conducted on a single supercapacitor module using battery test equipment and custom test plans. The performance of a supercapacitor module was investigated to confirm relevant specifications and to investigate dynamic performance in high-rate charge-discharge conditions. A time-series profile of SCESS operation from simulation results was used to confirm the supercapacitor module, as part of an SCESS, operated satisfactorily in the target application. The practical experiments were small-scale and low-cost; however they are representative of the overall performance of an SCESS stack. The results show that supercapacitor technology is suitable for the provision of several storage functions on an offshore wind turbine.

A cost-benefit analysis of the storage options in wind turbines was completed, considering an SCESS and rotor inertial storage. This indicated that the cost of an SCESS is expected to be less than 3% of the cost of a complete wind turbine, and that investment in an SCESS is economically viable provided that the resulting energy yield increase is over 1%. The positive results suggest that the next stage of research is justified, and areas for further research are described.

# Acknowledgements

This work was funded by The Engineering and Physical Sciences Research Council within the Supergen Wind Energy Technologies (Phase 2) consortium project, grant no. EP/H018662/1, 2010 – 2014.

The collaboration of partners in the Supergen Wind Energy Technologies Connection Theme is gratefully acknowledged. Particular thanks are due to Professor M. Barnes at the University of Manchester, and Dr B. Kazemtabrizi at Durham University.

# Table of contents

# 1 Introduction

Deliverable reports within the Supergen Wind Energy Project Theme 3, Task 3.4 Integration of storage, and Theme 4, Task 4.1 Offshore Connection set the scene for the cost-benefit analysis of storage options in wind turbines.

The reports included an overview of emerging Grid Codes, types of wind turbines, and offshore HVDC transmission, and highlighted the complexity of solutions required to provide frequency response, low-voltage ride-through (LVRT), and stability using storage. A literature review showed that there is no clear consensus about the storage capacity and choice of appropriate technology.

Rotor inertial storage is significant for large wind turbines, and can be made available by control of variable speed operation. Several researchers report that the loss of energy yield when using rotor inertia to provide short-term storage charge-discharge cycles is small. However, ensuring that there is available reserve from either rotor inertial storage or aerodynamic power could mean operating the wind turbine in sub-optimum conditions, resulting in a loss of revenue.

Three MSc projects at the University of Manchester investigated the inclusion of three storage technologies in DFIG wind turbines, namely supercapacitor, flywheel and battery storage systems.

The Supergen Wind reports concluded that electrical storage technologies should be considered alongside the use of rotor inertial energy, including investigation of size and technology. It was also concluded that supercapacitor technology was the most suitable for this storage application, and that the storage size (power and capacity), and overall system performance, should be investigated.

Development of a simulation model at Durham University included models of a 6MW wind turbine (incorporating a permanent-magnet synchronous generator), a full converter grid interface, with an energy storage system connected via the converter dc link. The detailed model included blade pitch control and variable speed operation, and enabled analysis of LVRT performance, and produced a power time-series under fault conditions.

This report investigated the feasibility of using a Supercapacitor Energy Storage System (SCESS) in wind turbines, including a cost-benefit analysis.

# 2 Requirements of an Energy Storage System

The requirements of the UK Grid Code for Fault ride through and the provision of frequency response are briefly summarised in Appendix A.

## *2.1 Low voltage ride-through*

This can be provided by rotor inertia by allowing surplus power to accelerate the rotor until pitch regulation can take effect. It is undesirable to reduce aerodynamic power rapidly as it results in torque transients and reduced power during a recovery period after the fault. For a large wind turbine where the inertia constant may be up to 10 seconds, storing the equivalent of rated power for 1 second would mean an increase in energy stored in the rotor inertia of 10%, with a corresponding rotor speed increase of around 5%. This is not a problem when the wind turbine is operating below rated speed. If the rotor speed increase becomes a problem when already operating near to rated speed, the converter may incorporate a braking chopper and resistor to protect the dc link from overvoltage.

## *2.2 Frequency response*

The UK Grid Code places requirements on offshore modules and generating units to meet a minimum frequency response specified in Appendix 3 of the Grid Code Connection Conditions. The frequency responses illustrated require the capability to ramp up during a 10s period to a power level during the period 10s to 30s for primary response, and during the period 30s to 30 minutes for secondary response. The contribution of an offshore energy storage system to frequency response is clearly limited to short periods, however it could provide an initial response that could assist by lowering the ramp time required of the wind turbine. In the case of primary and secondary frequency response to under frequency events, the requirement to provide a sustained power increase of at least 10% of operating power below 80% rated power means that a wind turbine operating below rated power must normally operate with a power reserve (i.e. the wind turbine power is pre-curtailed), considerably reducing the energy yield. Even when operating between 95 to 100% of rated power, wind turbines must be capable of some response, which could mean operating the power converters over rated power.

## *2.3 Inertial response*

The rate of change of frequency (RoCoF) can be high during a loss of generation event, particularly in island grids with high penetration of wind power. This is the case in Ireland, for example, where studies have shown that RoCoF values of greater than 0.5 Hz/s could occur and increased capability has been proposed[1] and decided[2]. In the UK a synthetic inertia response was proposed but is not yet included in the UK Grid Code. The proposed response is an increased power level that increases with the RoCoF and is a maximum of

[1] DS3 Rate of Change of Frequency Modification Recommendation to the CER. Available from: http://www.cer.ie/docs/000260/cer13143-(b)-rocof-recommendation-letter.pdf

[2] CER. Rate of Change of Frequency (RoCoF) Modification to the Grid Code. Available from: http://www.cer.ie/docs/000260/CER14081 ROCOF Decision Paper - FINAL FOR PUBLICATION.pdf

5.4% of nominal power for a RoCoF greater than 0.33 Hz/s. Although the emerging RoCoF requirements may not currently be provided by wind turbines, as penetration levels of wind power and other renewables increase, synthetic inertia requirements are likely to be introduced in national Grid Codes, and are already included in the European Draft Code.

## *2.4 Application of energy storage*

As already noted, rotor inertia is used in variable speed wind turbines, together with a resistive dump load in the converter dc link. However there are possible performance limitations and drawbacks, including torque transients and loss of energy yield. The requirement to provide frequency response is particularly costly as it may require pre-curtailment of up to 10%, depending on the operation power level. When wind turbines are operating at rated power, providing inertial response requires the power converters to be operated above rated power for the wind turbine, and this means they must be suitably rated. In any case, during the recovery period when the rotor speed has to recover to the optimum level, the power delivered to the grid must fall, and this is an undesirable result.

The GE Brilliant wind turbine platform uses battery energy storage connected to the DC link via a buck-boost converter to provide RoCoF response, a technique GE calls advance hybrid WindINERTIA. The deliverable report for Supergen Wind Task 2.1.2 Flexibility of operation[3] discusses current techniques for providing synthetic inertia by a wind turbine, and discusses how the GE WindINERTIA system works, although precise details of the control strategy have not been published. According to Burra (2014)[4] the justification for using storage rather than rotor inertia is that the rotor speed recovery after the response has performance implications in very high penetration grids. There is no further detail in the presentation of the storage power and energy specification or of the battery technology, however the WindInertia system is stated to be agnostic of storage chemistry and make. Several requirements such as short-term scheduling, ramp control and frequency regulation are listed, so it is possible that considerable battery capacity is envisaged with the economics improved by addressing multiple requirements. This may be economic where storage can be situated in a container on the ground adjacent to the wind turbine base, as illustrated in the presentation; however there are practical and economic difficulties in doing this offshore.

In this investigation we have focussed on the application to LVRT, frequency response and inertial response. However there are other benefits including power quality and stability improvement.

The required storage capacity to absorb power during a 3-phase dip is estimated to be around rated power times 0.4 to 0.8s, assuming that all the required response is provided by storage, without the use of rotor inertia and blade pitch control. To provide frequency response, an energy storage system with capacity of rated power times 1 second could provide a 5 second ramp up to 20% of rated power, followed by a 5 second ramp down to zero. Storage operated at a midpoint capacity level could provide both initial primary

[3] Supergen Wind Deliverable Report 2.1.2, Flexibility of operation, Adam Stock, September 2012
[4] R.Burra, Grid Performance – GE Brilliant Turbines, Presentation at EWEA conference, Barcelona, 2014

response response (by discharging the store) and high frequency response (by charging the store).

The estimate of usable storage capacity of 1 second at rated power provided a starting point for simulation studies to investigate the performance of various capacities of energy storage. Simulation studies in the Supergen Wind Energy project included modelling an individual wind turbine with variable rotor speed and blade pitch control, providing a response with contributions from rotor inertia and energy storage[5]. Energy storage could also be implemented at wind farm level. An earlier study by Kinko (2006) used a 3.8MJ supercapacitor bank (equivalent to around 12 seconds at 300kW) with a 300kW wind turbine to smooth power fluctuations due to wind turbulence.

[5] Supergen Wind Deliverable Report 4.1.8: Simulation of power systems, Behzad Kazemtabrizi, 2014

# 3 Supercapacitor energy storage system (SCESS)

## *3.1 SCESS specification*

Supercapacitors have reached a high level of design and market maturity. The global market in supercapacitors is large and increasing rapidly; it is expected to exceed $1billion in 2014 and increase by three times in the next four years[6]. Maxwell has been the world leader in supercapacitors, with sales approaching $100million in 2011, having increased five times in the preceding four years[7]. Maxwell's 16V and 75V modules are installed as backup power in blade pitch control systems in thousands of wind turbines worldwide, where the high reliability, low maintenance requirements, long lifetime, and a wide operating temperature range of -40 to +65°C are attractive attributes.

The electrical specification of modules from two manufacturers, Ioxus[8] and Maxwell[9], are shown in Table 1. Supercapacitor modules are constructed from several supercapacitor cells, for example the Ioxus 16V 58F module comprises six series-connected cells each with specification 2.7V 350F.

The energy stored in an ideal capacitor is calculated as $E = \frac{1}{2}\ C\ V^2$ Joules [Ws]. This is the maximum energy available at low discharge rates and in practice is an optimistic measure due to two factors:

- available energy can be significantly reduced at high discharge rates, due to the Equivalent Series Resistance (ESR) which acts like an internal resistance and results in a voltage drop at the supercapacitor terminals
- in most applications the operating voltage range is limited, e.g. for operation between $V_{rated}$ and 0.5 $V_{rated}$ the usable energy is 0.75 of the maximum energy available.

Assuming that supercapacitors are operated in the range 0.5 to 1.0 x rated voltage, the usable storage range is 0.75 x the total capacity at rated voltage. The energy store should be available to absorb and deliver similar amounts of energy; therefore the nominal voltage may be set to 0.79 x the rated voltage. The requirement to operate the energy store at high power, where a suitable limit for the ESR voltage drop could be 0.1 x the rated voltage, further increases the required storage capacity. Therefore the total storage capacity (at rated voltage) should be at least $4/0.75$ or 5.33 x the required usable capacity. This means that a charge or discharge capacity equivalent to 1 second at rated power would require a total capacity equivalent to 5.3 seconds at rated power, equivalent to 31.8MWs at 6MW. This total storage capacity can be realised by building various types of supercapacitor modules into a stack with rated voltage 2kV, as illustrated in Table 1.

[6] www.idtechex.com
[7] www.maxwell.com
[8] http://www.ioxus.com/ IMOD 16V/58F and 16V/500F modules
[9] http://www.maxwell.com/ 48V/165F and 56V/130F modules

| Single Modules | | | | |
|---|---|---|---|---|
| Manufacturer | Ioxus | Ioxus | Maxwell | Maxwell |
| Part No. | iMOD016V058 FP1M-00A | iMOD016V500 A22-01A | BMOD0165 P048 B09 | BMOD0130 P056 B03 |
| Voltage [V] | 16 | 16 | 48 | 56 |
| Capacitance [F] | 58 | 500 | 165 | 130 |
| ESR [mΩ] | 23 | 1.5 | 6.3 | 8.1 |
| Continuous Current [A] | 19 | 85 | 77 | 61 |
| Peak Current [A] | 200 | 2300 | 1900 | 1800 |
| Energy [Wh] | 2.13 | 18.2 | 52.8 | 56.6 |
| Volume [litre] | 0.594 | 4.4 | 14.5 | 21.1 |
| Mass [kg] | 0.76 | 5.1 | 13.5 | 18 |
| **Multi-Module stacks** | | | | |
| Series modules | 125 | 125 | 42 | 36 |
| Parallel modules | 30 | 4 | 4 | 4 |
| Total modules | 3750 | 500 | 168 | 144 |
| **Capacitance and ESR** | | | | |
| Capacitance [F] | 13.9 | 16.0 | 15.7 | 14.4 |
| ESR [mΩ] | 95.8 | 46.9 | 66.2 | 72.9 |
| Voltage [V] | 2000 | 2000 | 2016 | 2016 |
| **Power and Energy** | | | | |
| Max continuous power [MW] | 1.14 | 0.68 | 0.62 | 0.49 |
| Max peak power [MW] | 12.0 | 18.4 | 15.3 | 14.5 |
| Max energy [MWs] | 28.8 | 32.8 | 31.9 | 29.3 |
| Usable energy (0.5V to V) [MWs] | 21.6 | 24.6 | 24.0 | 22.0 |
| **Volume and Mass** | | | | |
| Volume [$m^3$] | 2.23 | 2.20 | 2.44 | 3.04 |
| Mass [kg] | 2850 | 2550 | 2268 | 2592 |
| **Volumetric and Gravimetric density** | | | | |
| W/l | 7400 | 8600 | 6331 | 4607 |
| Wh/l | 3.60 | 3.60 | 3.63 | 2.64 |
| W/kg | 5800 | 9900 | 6800 | 5400 |
| Wh/kg | 2.8 | 4.1 | 3.9 | 3.1 |

Table 1. Examples of Supercapacitor Module and Proposed Multi-Module Stack specifications

The parameters of the stack are calculated using the manufacturer's module specifications. For example, the maximum peak and continuous power of the stack are simply calculated using the maximum peak and continuous currents specified by the manufacturer, times the rated voltage. The maximum peak current is generally calculated at the impedance-matched power level. Supercapacitors are ideally suited to applications requiring high power for a short duration, and the specified maximum peak power illustrates the power level that the module is ultimately capable of, with reduced energy capability. While the maximum peak power may not be directly relevant, the maximum continuous power is a safe guideline. It should be noted that for a maximum ESR voltage drop of 0.1 x rated voltage, in the case of the stack using the Ioxus 16V / 58F module, the maximum stack current is 2,087A, or 69.6A per module. This means the maximum power of the stack would be around 4MW at 2kV, although in practice the maximum power will depend on the cell voltage operating point. It is clear that the value of the ESR is an important design consideration, and Table 1 shows stacks using other modules that have much lower values of ESR. Although it is clear that the Ioxus 16V / 58F module is not necessarily the best choice for use in the multi-module stack, the module was a suitable size for use in small-scale experimental tests.

Manufacturer's data states that the capacitance decreases by a maximum of 30% and ESR increases by a maximum of 100% after 10 – 14 years at rated voltage and 25°C operating temperature. This degradation is a significant problem and would result in a significant decrease in performance during a ten year lifetime, and means the initial design would need to be over-specified. Efforts should be made to maintain the operating temperature as low as practicable, and this should be possible in a UK offshore installation.

Supercapacitor cells typically have a capacitance tolerance in the range -10% to +20% of nominal capacitance. When cells are operated in series the disparity in capacitance values affects the final voltage distribution when the module is fully charged, resulting in cell voltages in the range +11 to -17% of the nominal voltage. The problem can become more acute for large numbers of cells in series, depending on the distribution of cell capacitance. The risk is that some cells may be overcharged resulting in faster ageing and deterioration of capacitance and internal resistance. A further problem is encountered in a series stack that remains on trickle charge for a long period, when variation in cell leakage current results in voltage unbalance. Generally cells in modules are chosen to be matched, and an active or passive balancing circuit is included. The Ioxus 16V 58F modules have passive balancing circuits consisting of 120 Ω resistors connected in parallel with each cell, which increases the module leakage current to 22mA, dominating the cell leakage current of <1mA. This results in a resistive power loss of 0.35 W per module, or 1.33 kW for the stack of 3,750 modules. A maximum of 48 Ioxus modules can be series-connected to give a stack voltage of 750V, while additional balancing would be required in a 2kV stack.

The packing densities of modules are significantly lower than the cylindrical cells densities, due to additional balancing circuits, interconnections and terminals. For example the Ioxus 16V 58F module has volumetric density reduced to around 64% and gravimetric density reduced to around 55% of the respective densities of the constituent cells, as shown in Table 2.

| | | | Volumetric density | | Gravimetric density | |
|---|---|---|---|---|---|---|
| **Supercapacitor manufacturer** | **Voltage** | **Farads** | **W/l** | **Wh/l** | **W/kg** | **Wh/kg** |
| Ioxus cell | 2.7 | 350 | 11,000 | 5.9 | 10,000 | 5.4 |
| Ioxus 6-cell module | 16 | 58 | 7,400 | 3.6 | 5,800 | 2.8 |

Table 2. Comparison of supercapacitor cell and module volumetric and gravimetric densities

## *3.2 SCESS model parameters*

The specification of an SCESS stack using 3,750 Ioxus 16V 58F modules has parameters as shown in Table 3.

| | |
|---|---|
| Capacitance | 13.9 Farad |
| ESR | 95.8 mΩ |
| Maximum Voltage | 2000 V |
| Max Continuous Power | 1.1MW |
| Maximum peak power (1s) | 12.0 MW |
| Max usable storage capacity (0.5V to V) | 21.6 MWs |

Table 3. SCESS stack parameters for a simulation model

Detailed models of simulation models have been well described in the literature, for example by Shi (2008). These range from a simple model incorporating an ideal capacitor and series resistor (with value equal to the ESR), to those simulating high frequency dynamics by incorporating parallel branches with different time constants. The single time-constant model with capacitance 13.9F and ESR 95.8 mΩ was proposed for simulation. The single time-constant approach is also described by Korakitis (2012) in his thesis.

Experimental tests were conducted to assess the performance of a single Ioxus 16V 58F module, and to confirm that the single time-constant simulation model is adequate for representing the dynamic response required in the target application. Operation in the target application was successfully demonstrated as described in the next Section, and tests to evaluate module performance are described in Appendix C.

# 4 Validation of the SCESS simulation results

## *4.1 Storage parameters in the simulation model*

Development of a model of a 6MW permanent magnet wind turbine has been described by Kazemtabrizi (2014). In addition to an SCESS, rotor inertia was considered as a storage option and the energy available depends on the rotor inertia and rotor speed range as well as the particular operating conditions. The SCESS model parameters were defined in the previous section. Manufacturers' specifications generally do not include the rotor moment of inertia, and the blade and rotor mass distributions that would be required to perform an analytical derivation are not available. Therefore relationships based on trends were developed, and calibrated using a reference machine, and this is described in Appendix D. Parameters for the Siemens SWT-6-154 6MW wind turbine are described in Table D3, Appendix D, where the key storage parameters are the rotor speed range of 5 – 11 rev/min (0.53 – 1.15 rad/s), and the derived inertia time constant of 7.82 seconds.

## *4.2 Experimental validation of the SCESS performance*

A result from simulation studies of the power absorbed in the SCESS during a single-phase fault of approximately 100ms duration is shown in Figure 1.

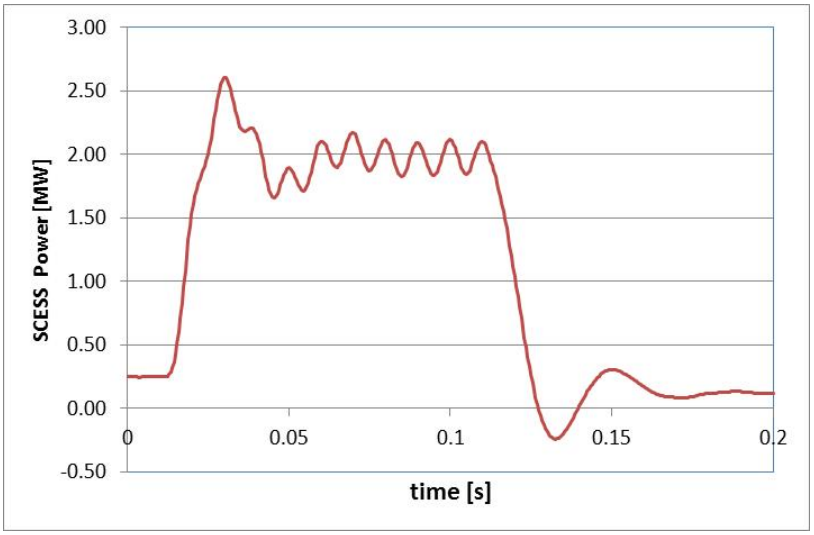


Figure 1. SCESS power profile from simulation[10]

The profile of around 2 MW power absorbed by the SCESS with 3,750 modules is equivalent to around 533 W per module. The nominal operating point of the modules is set to 12V, around the middle of the operating range so that the SCESS would be capable of absorbing or delivering power. In this case the module current required is nominally 44A, in excess of its continuous current rating of 19A but well within its 1 second peak power rating.

[10] Supergen Wind Deliverable Report 4.1.8: Simulation of power systems, Behzad Kazemtabrizi 2014

Experimental results using a 5ms timestep (Figure 2), show that the module is capable of absorbing the power step. The voltage is a function of the charge gained and voltage drop in the ESR, and shows a net increase over the period. The energy absorbed was calculated from the measured voltage and current, and is 65 J at the end of the 200ms period, less than 1% of the theoretical maximum capacity. Taking energy lost in the ESR into account, the charge efficiency was calculated as 92.5%.

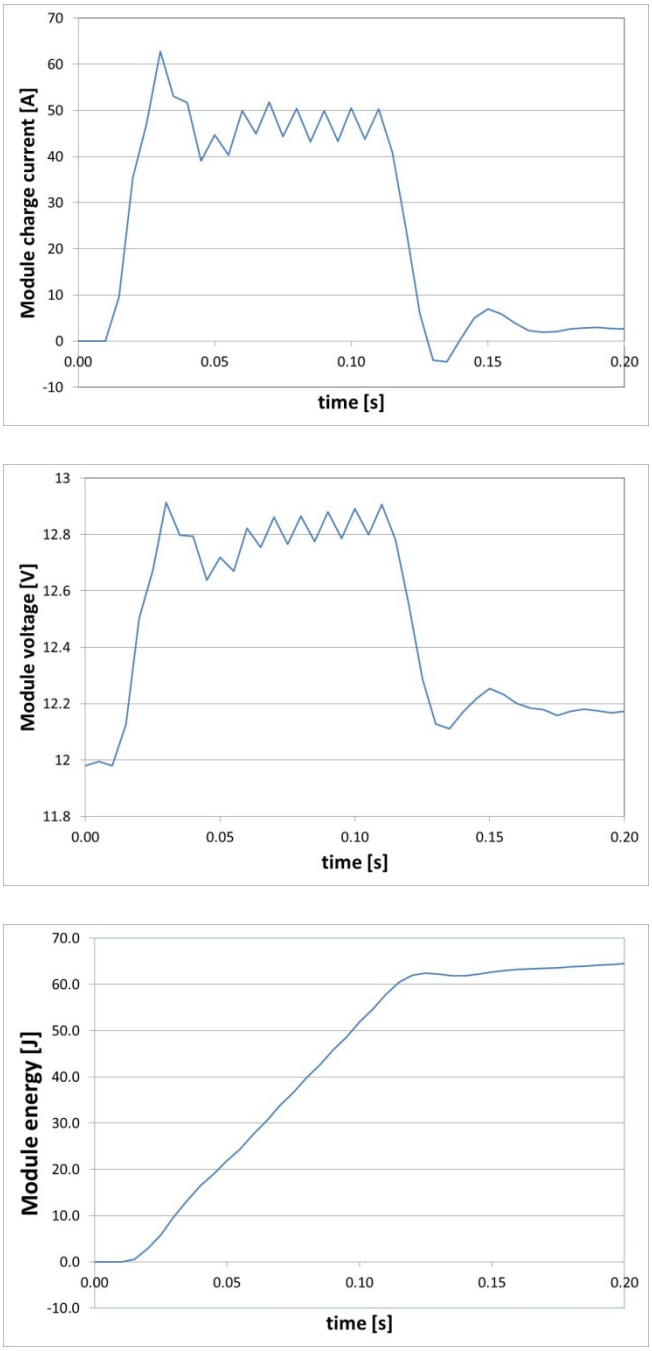


Figure 2. SCESS module response to a power step
a) current, b) voltage, c) energy

# 5 SCESS Costs

## *5.1 Supercapacitor cost*

The current cost for low quantities of supercapacitor modules purchased from distributors is still high, of the order of 60 £/Wh, while the cost for low quantities of cells is in the region of 20 £/Wh.

Information obtained direct from one manufacturer in 2014 indicates that much lower prices are possible, depending on quantity, as shown in Table 4. It should be noted that these prices are market prices, not necessarily that of Ioxus only. The currency exchange rate when the data was obtained in 2014 (and used in the price conversion) was US$ 1.66 = UK£ 1.00. Additional information from manufacturers at that time suggested a continuing price reduction of from 5% to 12% per year, depending on the cell type, module type and quantity. Prices had reduced approximately 99% over the past 10 years. Future supercapacitor price reduction depends on market growth and increasing production automation.
A review of prices in April 2017 revealed that in US$ terms, module prices have generally reduced by 5% per annum, and by significantly more for some modules. However there has been a significant change in exchange rate since March 2014, tending to increase module prices in UK£ terms.

| | V | Farad | Wh | US$ | | US$/Wh | | UK£/Wh | |
|---|---|---|---|---|---|---|---|---|---|
| | | | | From | To | From | to | from | to |
| **single cell** | 2.7 | 1 | 0.001013 | $0.005 | $0.015 | $4.94 | $14.81 | £2.97 | £8.92 |
| **module** | 48 | 165 | 52.80 | $700 | $1,200 | $13.26 | $22.73 | £7.99 | £13.69 |
| **module** | 16 | 500 | 17.78 | $250 | $550 | $14.06 | $30.94 | £8.47 | £18.64 |
| **module*** | 96 | 83 | 106.24 | $1,300 | $2,100 | $12.24 | $19.77 | £7.37 | £11.91 |

Table 4. Volume prices of supercapacitor cells and modules[11] (*rack-mountable)

This suggests that the cost of high quantities of supercapacitor modules could be as low as around 8 £/Wh, and that the total cost of supercapacitor modules for the SCESS could be in the region of £63,900.

## *5.2 Power converter cost*

The bi-directional DC-DC power converter could have a high cost, weight and volume, and an appropriate method of interfacing should be chosen. Cihak (2011) described three methods of interfacing a supercapacitor stack to a DC link, direct (or passive); non-isolated DC-DC converter; and isolated DC-DC converter. According to Cihak (2011) supercapacitors have been connected directly to DC-links in some low-power applications; however this does not seem feasible in high power applications where the AC currents would cause

[11] Private communication with Chad Hall, co-founder and VP of Ioxus Inc., 11th March 2014

unacceptable heating due to the ESR and a short lifetime is likely. A buck-boost DC-DC converter is likely to be the most cost-effective solution, and this type has been used to interface the SCESS in the Task 4.1.8 model.

A full-power AC-AC converter is used in wind turbines with a permanent magnet synchronous generator. An estimate of the cost of such converters can be obtained by looking at the breakdown of costs in offshore wind power systems. Ranges of capital investment and wind turbine costs are presented in a report by IRENA (2012), see Table 5, where the average offshore wind turbine cost may be around 1,575 $/kW. The report used data from various sources (with various currency exchange rates) and acknowledges that exchange rate fluctuations can have a significant impact on project costs.

| | Onshore | Offshore |
|---|---|---|
| Capital investment costs of wind power systems | 1,700 to 2,450 $/kW | 3,300 to 5,000 $/kW |
| Wind turbine cost share | 84 to 65 % | 50 to 30% |
| Implied wind turbine cost | 1428 to 1592 $/kW | 1650 to 1500 $/kW |

Table 5. Capital Cost of wind power systems, using data from IRENA (2012)

Analysis by Douglas-Westwood (2010) resulted in an offshore wind turbine cost of 11.9 kNOK/kW (1,983 $/kW using an historical exchange rate of NOK 6 = USD 1. Therefore wind turbine costs may be in the region 1,575 to 1,983 $/kW, and assuming the power converter share of the wind turbine cost is 5.01% (see footnote[12]), the power converter would cost in the region of 78.9 to 99.3 $/kW. A report by Tegen (2013), reviewing the cost of wind energy in 2011, states that the variable-speed electronics cost in an onshore wind turbine is 108 $/kW. An earlier report by Fingersh (2006) used a figure of 79 $/kW, drawing on a detailed analysis of component costs by Poore (2003). Using a cost of £100 $/kW and an historical exchange rate of US$ 1.66 = UK£ 1.00, results in a cost of 60 £/kW, and a cost of £360k for a 6MW converter. Considering the respective number of power electronics devices used, the cost of a buck-boost DC-DC converter may be expected to be considerably less than a full power AC-AC converter, possibly in the region of £100k.

## *5.3 Other SCESS costs*

Other SCESS construction costs include supercapacitor module mounting and interconnection, and a cabinet for the whole assembly.

Mounting and interconnection of cells into modules results in a cost multiple of 2 to 3 times the cell costs, see Table 4. Interconnecting a large number of small modules is likely to incur a significant cost. However rack-mountable modules with energy 106 Wh are available at around 8 £/Wh, see Table 4, and around 75 of these would be required to construct an

[12] Supply Chain: The race to meet demand, Wind Directions, pp27-34, January/February 2007

SCESS. The cost of mounting and interconnecting a small number of large modules is likely to be lower than for small modules, and a cost of £10,000 is assumed.

The total volume of the small modules comprising the SCESS is 2.23 $m^3$ and the mass is 2,850 kg (from Table 1), however this clearly understates the practical packing density. Increases of 100% for the volume, and 50% for the mass give an estimate of the constructed SCESS volume and mass as shown in Table 6.

The volume and mass of the SCESS power electronics converter should be added to this. It is also useful to compare the SCESS volume and mass with the ABB PCS 6000 medium voltage full power converter, with selected parameters as shown in Table 7. Although a specification for the SCESS power electronics converter is not currently available, the complete SCESS plus converter may well be double the estimates in Table 6 of volume and mass for the SCESS alone.

| | Modules only | Constructed SCESS | | Siemens SWT-6.0-154 |
|---|---|---|---|---|
| | From Table 1 | Possible increase | Estimated | Nacelle |
| Volume | 2.23 $m^3$ | 100% | 4.46 $m^3$ | 498 $m^3$<br>(15m long, diameter 6.5m) |
| Mass | 2,850 kg | 50% | 4,275 kg | Approximately 200 tonnes<br>(top head weight 360 tonnes) |

Table 6. Volume and weight of the SCESS capacitors, and the Siemens SWT-6.0-154 nacelle[13]

| | |
|---|---|
| Converter voltage | 3.3 kV |
| Number of IGCT[14] semiconductors in converter | 24 |
| Braking resistor capacity | 15MJ / 30MJ |
| Number of IGCT semiconductors in chopper | 2 |
| Volume | 15.3 to 16.8 $m^3$ |
| Mass | ~ 6,200 kg |

Table 7. Selected specifications for the ABB PCS 6000 medium voltage full converter

The Siemens SWT-6.0-154 nacelle volume and weight are also shown in Table 6 to put the SCESS volume and weight in perspective, where the shares of costs of a wind turbine for the nacelle and tower are in the region of 2% and 25% respectively. An increase in nacelle volume and mass would be in the region of 1% and 2% respectively and installing the SCESS in a larger nacelle could result in a significant increase in the total wind turbine cost, possibly in the region of 0.5% to 1% i.e. around £45k for a 6MW wind turbine.

[13] http://www.siemens.com/press/pool/de/feature/2013/energy/2013-01-rotorblade/factsheet-6mw-e.pdf
[14] IGCT – Integrated gate-commuted thyristor

However it should also be noted that the ABB PCS 6000 converter is designed for installation within the base of the wind turbine tower, and it seems reasonable to assume that the SCESS including its converter could also be installed on another level near the base of the tower. In this case a much lower cost of £10k is assumed for installation.

### *5.4 Summary of SCESS costs*

A large number of assumptions have been made when estimating costs. In particular there is a low level of confidence in the estimated cost of the DC-DC power converter, and this is the dominant cost, see Table 8.

| Component | Cost |
|---|---|
| Supercapacitor modules | £63,900 |
| Power converter | £100,000 |
| Other costs | £20,000 |
| **Total** | **£183,900** |

Table 8. Summary of initial estimate of SCESS capital costs

# 6 Cost and benefits

Here we consider the costs and benefits of using rotor inertial storage and an energy storage system. Ideally the control and operation of a wind turbine incorporating both forms of storage should be studied in detail using simulation studies, and the model developed in the Supergen Wind Energy project, Kazemtabrizi (2004), is sufficiently detailed to allow this to be done.

Simulation results obtained in Task 4.1.8 for the operation of the SCESS have demonstrated operation under fault conditions, and the simulated SCESS power time series has been tested experimentally at a small scale. This means that there is now a high degree of confidence that an SCESS could be implemented, and would satisfy the requirements.

The purpose of the cost-benefit analysis is:

a. To determine if the capital expenditure of an SCESS is a sound investment
b. To provide a basis for comparing options

The data required is the capital expenditure, operation and maintenance, and revenue over time, and the following assumptions have been made.

Capital expenditure: £185k in year 0 for the full SCESS, and £65k after 15 years for the complete replacement of the supercapacitor modules.

Revenue: This is in the form of an additional energy yield, assuming that the inclusion of an SCESS instead of rotor inertia allows the wind turbine to operate closer to its optimum operating point, resulting in additional energy yield. This additional yield has not yet been demonstrated by simulation results; therefore a level of 1.5% has been used, based on an assessment of performance reported in the literature (see Appendix B). The additional yield is valued at the strike price per kWh paid according to the year of installation or commissioning.

Strike price: £155 for 2014/15. The strike price for offshore wind for 2014/15 to 2018/19 is from the Electricity Market Reform Delivery Plan (2013), see Table 9.

| Technology \| Year | 2014/15 | 2015/16 | 2016/17 | 2017/18 | 2018/19 |
|---|---|---|---|---|---|
| Offshore Wind £/MWh | 155 | 155 | 150 | 140 | 140 |

Table 9. Strike price for offshore wind
(Data from Electricity Market Reform Delivery Plan 2013, page 37)

Standby losses:
As noted earlier, the loss due to the SCESS balancing resistors is 1.33kW. Further balancing circuits would be required for an SCESS voltage in excess of 750V. The supercapacitor stack voltage could be maintained by an auxiliary supply to avoid using the buck-boost power converter and to reduce power electronic losses; however the power converter would have

to remain on standby. Insufficient information is available to make an accurate estimate of standby losses, and a figure of 5kW is assumed, resulting in energy loss of 43,800 kWh/year. It is noted that the ABB PCS 6000 full-power converter uses auxiliary power of 12kW. This is mainly for the liquid cooling circuit, to remove converter losses of 120kW (for specified 98% efficiency) when operating at 6MW.

Operating losses:
For a total of 20 full cycle events per year, each with energy loss in the SCESS of 6MWs (assuming the worst-case impedance-matched load), the total operating loss would be 33kWh/year.

Capacity factor: 38% as used in the Offshore Wind Assessment in Norway (2010). The factor used in various other analyses ranges from around 34% to 40%.

Discount rate: 7% as used in the Offshore Wind Assessment in Norway (2010).

The key parameters are summarised in Table 10 and define the reference case.

| | |
|---|---|
| Energy price | 155 £/MWh |
| Capacity factor | 38% |
| Energy yield increase | 1.5% |
| SCESS capital cost | £185,000 |
| Discount rate | 7% |
| Project period | 20 years |

Table 10. Summary of parameters used in the NPV calculation

A standard procedure was used for calculating the net present value (NPV) of the time series of cash flows, expenditure and income. The NPV(i) of each cash flow at time t, where $R_t$ is the cash flow at time $t$ , and $i$ is the discount rate, is:

$$NPV(i) = \frac{R_t}{(1+i)^t}$$

The total NPV is the sum of all cash flows:

$$NPV(i,N) = \sum_{t=0}^{N} \frac{R_t}{(1+i)^t}$$

The NPV of the SCESS for project periods up to 30 years is shown in Figure 3, showing that the NPV for the reference case with 20 year period is just over £200k (or in other terms, 35 £/kW installed wind power). Allowing for the uncertainties, this suggests positive economic benefits of investment in an SCESS. One way to assess this is to compare the SCESS investment case with the investment case for offshore wind turbines using the same level of finance. Clearly there is a wide spread of project finances depending on location offshore,

and this would have to be assessed on a case-by-case basis. An investigation within the Supergen project[15] presents an analysis of the costs of UK offshore wind energy.

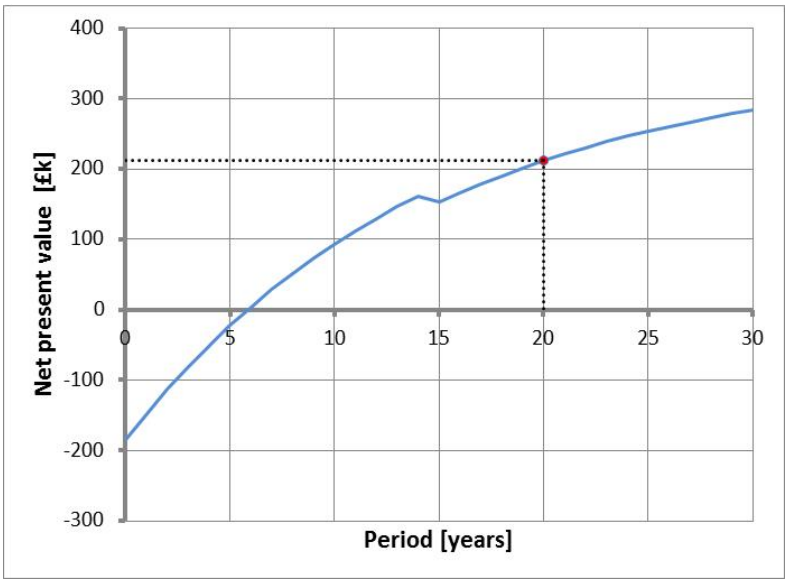


Figure 3. Net Present Value of SCESS for project periods up to 30 years

Given that confidence is low in some of the values of parameters, particularly the energy yield increase, a sensitivity analysis has been done for each parameter, assuming that the other parameters remain constant at the reference values, see Figure 4. There is a drive to reduce the cost of offshore wind energy (by reducing wind turbine capital, installation and operation costs) in future years, beyond the prices already set for the next few years, as shown in Table 9, and it is clear this would have a large impact on the SCESS NPV. However the capital cost of the SCESS power converter and supercapacitors may also decrease with time and this would increase the NPV, although it is not particularly sensitive to the capital cost. However the NPV is very sensitive to the energy price, discount rate, and capacity factor; fortunately these are generally predictable or known at the planning stage.

It is not surprising that the NPV is particularly sensitive to the assumed energy yield increase, as this is the sole source of income in the analysis. At the same time there is low confidence in the value assumed. However the NPV sensitivity analysis clearly shows that the yield increase should be greater than around 1% for the SCESS to be commercially viable.

[15] Supergen Wind Deliverable Report 4.2.5 Assessment of UK economically accessible offshore wind resource (2014)

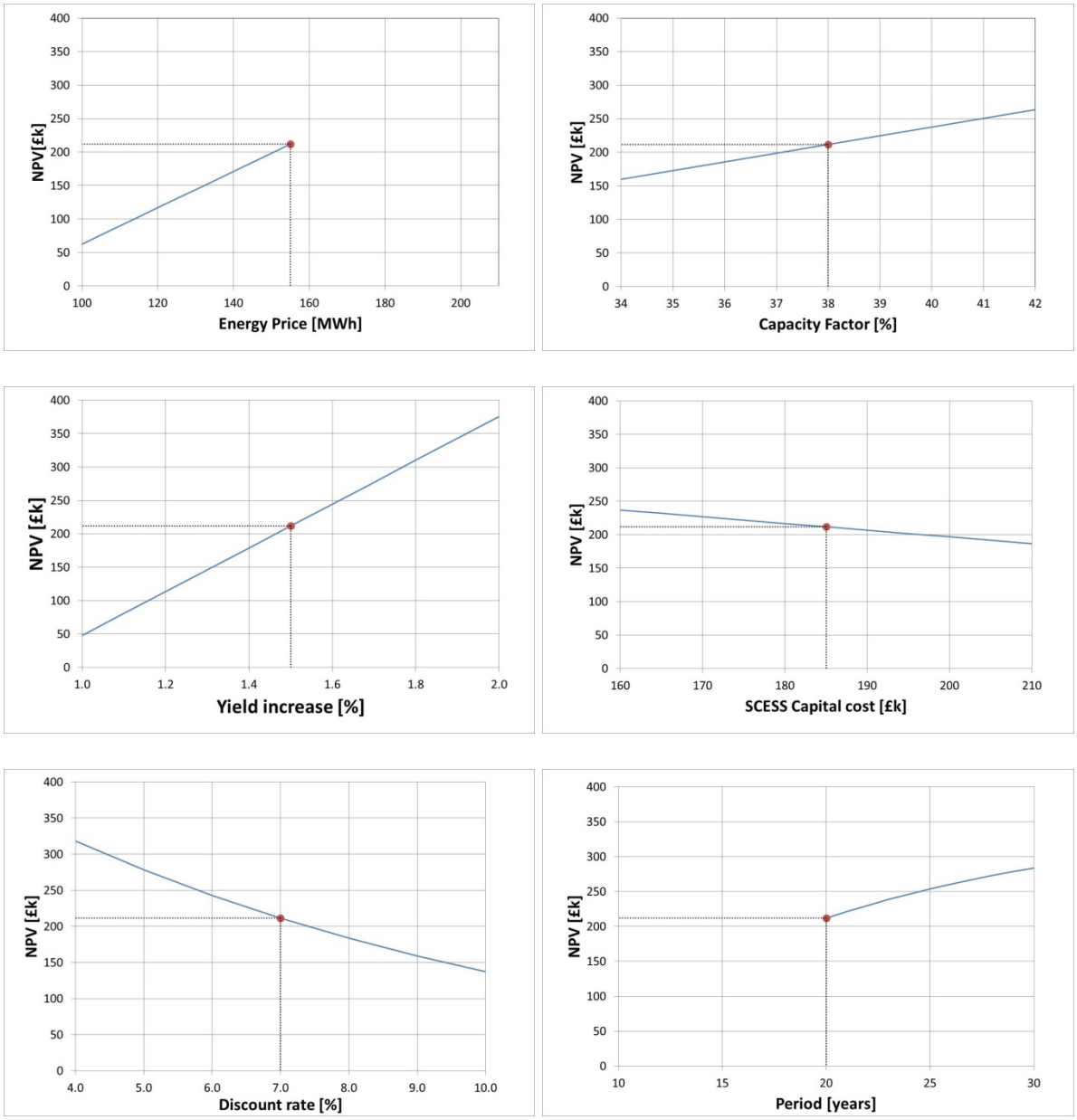


Figure 4. Sensitivity of the NPV to energy price, capacity factor, energy yield increase, capital cost, discount rate and project period.

# 7 Conclusions

The experimental tests confirm the simulation results, and show that a supercapacitor stack is an attractive technology for the provision of several storage functions on an offshore wind turbine. In particular, the SCESS has the potential to provide inertial response, a requirement that is under consideration and is likely to be specified in future revisions of national Grid Codes.

The analysis suggests the cost of an SCESS may be less than 3% of a complete wind turbine cost, and a cost-benefit analysis indicates that investment in an SCESS is economically viable provided that the resulting energy yield increase is over 1%.

It should be noted that a large number of assumptions have been made when estimating costs and cost-benefit parameters. Many of the costs in the analysis used historical exchange rates, and it is clear that exchange rate fluctuations can have a significant impact on project costs, and further investigation is necessary for future projections.

The positive initial results suggest that the next stage of research is justified, including several topics. It is suggested that the technical aspects of an SCESS implementation be considered in detail, including the optimum stack voltage and any additional balancing circuits, and the buck-boost power electronic converter design and control. The sizing of an SCESS and the control of both rotor inertial storage and an SCESS to optimise performance should be investigated. The yield increase resulting from the inclusion of an SCESS should be investigated by further simulation studies. Finally long term experimental tests are recommended to investigate the degradation in capacitance and ESR of supercapacitors when maintained at a high state of charge.

# 8 References


Cihak, E.E.T., Jakopovic, E.E.Z., (2011). Supercapacitors in power converter DC link: A short overview of design and application issues, *MIPRO, Proceedings of the 34th International Convention*, Opatija, May 2011.

Department of Energy and Climate Change (2013). *Electricity Market Reform Delivery Plan*, URN: 13D/343, December 2013 [Available from: https://www.gov.uk/government/publications/electricity-market-reform-delivery-plan ]

Fingersh L., Hand M., Laxson A., (2006) Wind turbine design cost and scaling model, *NREL Technical Report NREL/TP-500-40566*, December 2006.
[Available from: http://www.nrel.gov/docs/fy07osti/40566.pdf ]

Hogg S., & Crabtree C. ed. (2016) *UK Wind Energy Technologies* ISBN 978-1-13-878046-0, Abingdon,Oxon, Routledge, 2016

Kazemtabrizi B, Hogg S., (2014). A new simulation and control model for a variable speed variable pitch direct drive large offshore wind turbine generator with integrated energy storage, *ASME Turbo Expo 2014, Düsseldorf, Germany*, June 16–20, 2014

Kinko T., Senjyu T., Urasaki N., (2006). Output levelling of renewable energy by electric double-layer capacitor applied for energy storage system. *IEEE Transactions on Energy Conversion*, Vol.21, No.1, March 2006

Korakitis K. (2012) *Modelling of a large doubly-fed induction generator wind turbine integrating energy storage system*, MSc dissertation, University of Manchester, 2012

The Research Council of Norway (2010) *Offshore Wind Assessment in Norway*, Douglas-Westwood, Oslo, (2010)
[Available from: http://www.forskningsradet.no/ ]

Poore R., Lettenmaier T., (2003) Alternative Design Study Report: WindPACT advanced wind turbine drive train designs study, *NREL Report NREL/SR-500-33196*, August 2003.
[Available from: http://www.nrel.gov/docs/fy03osti/33196.pdf ]

Renewable Energy agency (IRENA) (2012). *Renewable Energy Cost Analysis - Wind Power*.
[Available from: http://www.irena.org/ - Publications – Reports and Papers ]

Shi L., Crow, M.L., (2008) Comparison of ultracapacitor electric circuit models, *IEEE Power and Energy Society General Meeting - Conversion and Delivery of Electrical Energy in the 21st Century*, 20-24 July 2008

Tegen S., Lantz E., Hand M., Maples B., Smith A., Schwabe P., (2011) Cost of Wind Energy Review, *NREL Report NREL/TP-5000-56266*, March 2013
[Available from: http://www.nrel.gov/docs/fy13osti/56266.pdf ]

The Grid Code, Issue 5, Rev.3 April 2013. National Grid Electricity Transmission plc. Available from: http://www2.nationalgrid.com/uk/industry-information/electricity-codes/grid-code/the-grid-code/

# A. Appendix: Summary of UK Grid code requirements

Fault ride through. The requirements to withstand voltage dips on the onshore transmission system operating at Supergrid voltage may be met either at the Supergrid connection point (Grid code[16] Section CC.6.3.15.1) or at the LV side of the Offshore platform (Grid Code section CC.6.3.15.2). In each case the requirements to withstand dips up to 140ms, and greater than 140ms are specified. Addressing the requirements at the LV side of the offshore platform is the logical choice for the offshore wind study, when assessing the contribution of rotor inertia and additional energy storage in wind turbines.

The Grid Code Iss 5 section CC.6.3.15.2 (a) shows the voltage profile limits applicable at the LV side of the Offshore Platform for voltage dips up to 140ms, while section CC.6.3.15.2 (b) shows the voltage profile limits for dips greater than 140ms.

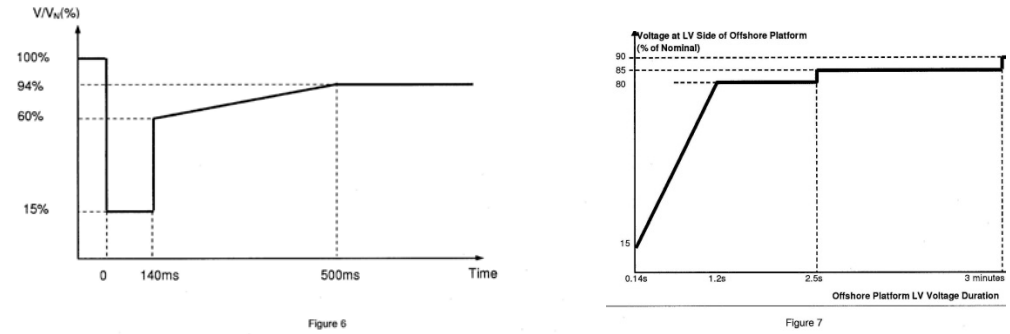


Figure A.1. LVRT voltage profile limits
(extract from Grid Code Iss 5 section CC.6.3.15.2, Figures 6 and 7)

Frequency response. The Grid Code Section CC.6.3.7 places requirements on offshore modules and generating units to provide frequency response, as specified in Connection Conditions Appendix 3. The primary / secondary / high frequency responses to a 0.5Hz step require the capability to increase power (P and S response), and to reduce power (H response). The minimum power response (usually 10% of Registered Capacity) depends on the operating conditions, and is specified by a requirement profile (Fig CC.A.3.1 Appendix 3).

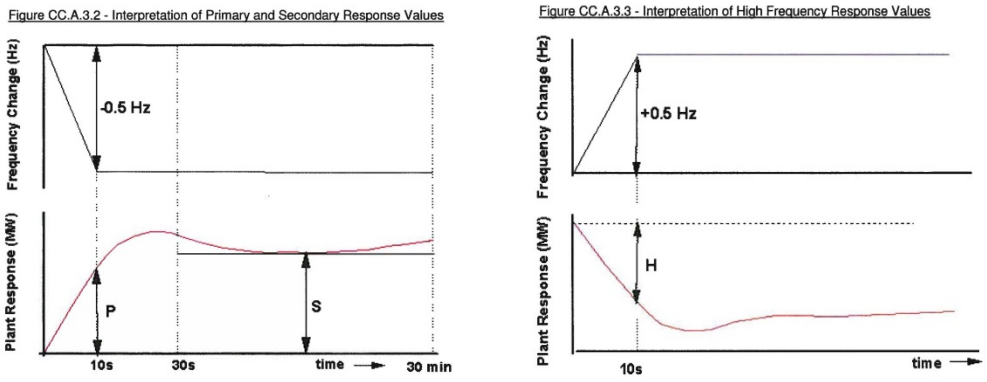


Figure A.2. Primary / Secondary / High frequency response
(extract from Grid Code Iss 5, Connection Conditions, Appendix 3)

[16] The Grid Code, Issue 5. National Grid Electricity Transmission plc.
http://www2.nationalgrid.com/uk/industry-information/electricity-codes/grid-code/the-grid-code/

# B. Appendix: Review of research into energy yield loss

Supergen Wind Deliverable report 4.1.7 (2012) included a literature review of investigations into requirements for LVRT, frequency regulation, synthetic inertia, as stated in Grid Codes, and the operation of wind turbines. Here we revisit this to see if there is a consensus on the possible loss of energy yield resulting from meeting the Grid Code requirements using rotor inertia.

A method for analysis of the available rotor kinetic energy for a range of wind speeds, and the loss of energy capture, when the wind turbine is operated using de-rating to increase the size of the power reserve is described by Rawn (2009, 2010). The trade-off between potential revenue from kinetic energy and the loss of energy capture is examined.

At lower wind speeds (and lower rotor speeds) the usable inertial storage (when delivering power) is reduced because of the lower rotor speed limit. Although this can be compensated by operating the wind turbine at a higher rotor speed, the operational losses can be high, as described by De Haan (2011).

Control strategies for an inertial controller were investigated by Wu (2011, 2012), concluding that an improved response (instead of an ideal response as would be provided by a synchronous generator) could provide smoother power response, shorter recovery period, and less energy loss.

Within the Supergen Wind project, Stock (2012, 2014) investigated a method for providing frequency response using an additional outer feedback loop (power-adjusting controller, PAC) to augment the central controller. Simulations demonstrated the effectiveness of the controller in responding to frequency drops, utilising a small proportion of stored energy equivalent to around 1 p.u. for 0.3s. The aerodynamic power loss during the simulated event was found to be less that 1%. Stock (2014) also investigated the use of the PAC for providing frequency droop response, which normally results in a reduction in energy capture due to pre-curtailment. Simulations showed the reduction in energy capture ranged from 10.91% to 3.18% depending on the wind regime and PAC strategy. The Deliverable report 2.1.2 describes a controller that effectively provides synthetic inertia, and features to ensure the operation is within safe torque and rotor speed envelopes, resulting in some performance limitations.

Also within the Supergen Wind project, Anaya-Lara et al (2014) describes simulation studies on a DFIG wind turbine providing frequency support. The example shown is of a wind turbine initially operating at 0.7pu torque. Releasing kinetic energy and reducing the rotor speed results in a reduction of energy provided by the rotor, and to mitigate this effect the rotor speed is slowly increased back to its original value.

The synthetic inertia proposal for the UK Grid Code was described by Licari (2013) with simulation results of a wind turbine with inertia coupling demonstrating improvement by utilising additional DC link capacitance. Assuming that a typical DC link capacitance of 58,000 µF operated at 2kV has storage capacity 116kJ, the DC link capacitance could not normally

make a significant contribution to the response. Zeni (2013) and Moore (2012) describe how wind turbines could provide synthetic inertia.

Several of these investigations mention the loss of energy yield resulting from the use of rotor inertia, however in general this is not quantified.

## *B.1 References to Appendix B*


Anaya-Lara O., Luque A., Adam G.P., Campos-Gaona D., (2014) Dynamic Performance assessment, *Supergen Wind Deliverable Report 4.1.4*, January 2014

de Haan J.E.S., Frunt J.E., Kling W.L., (2011) Wind Turbines Kinetic Energy Storage Potential for Frequency Support, *EWEA Conference*, Brussels, 14-17 March 2011

Licari J., Ekanayake J., Moore I.,(2013) Inertia response from full-power converter-based permanent magnet wind generators, *J. Mod. Power Syst. Clean Energy*. pp 26-33, 2013

Moore I.F., (2012) *Inertial Response from Wind turbines*, PhD Thesis, Cardiff University, 2012. Available from: http://orca.cf.ac.uk/42939/2/Inertia Response from Wind Turbines.pdf

Rawn B.G., Lehn P., Rogers E.S., (2009) A method for assessing stability of wind turbines providing grid frequency stabilization, *Nordic Wind Power Conference* 2009

Rawn B.G., Gibescu M., Kling W.L.,(2010) A Static Analysis Method to Determine the Availability of Kinetic Energy from Wind Turbines, *IEEE Power And Energy Society General Meeting*, 2010

Stock A., Leithead W., (2012) Providing grid frequency support using variable speed wind turbines with augmented control, *EWEA Conference*, Copenhagen, 16th – 19th April 2012

Stock A., Leithead W., Pennock S., (2014) Providing Frequency Droop Control Using Variable Speed Wind Turbines with Augmented Control. *EWEA Conference*, Barcelona, March 2014

Stock A., (2012) Flexibility of operation, *Supergen Wind Deliverable Report 2.1.2*, September 2012

Wu L., Infield D., (2011) Modelling the provision of inertial response from variable speed wind turbines, *IET Conference on Renewable Power Generation (RPG 2011)*, Edinburgh, UK, 6-8 Sept. 2011

Wu L., Infield D., (2012) Wind plant contributions to power system frequency response, *EWEA Conference*, Copenhagen, 16th – 19th April 2012

Zeni L., Rudolph A.J., Münster-Swendsen J., Margaris I., Hansen A.D., Sørensen P., (2013) Virtual inertia for variable speed wind turbine. *Wind Energy* Vol 16, Iss 8, pp. 1131–1309 2013 [Available from DOI: 10.1002/we.1549 ]

# C. Appendix: Evaluation of supercapacitor module performance

Selected test procedures[17,18,19] were conducted to evaluate the performance of the Ioxus 16V 58F module, shown in Figure C.1.b). The test equipment used was a BaSyTec[20] battery test system fitted with an 18V / 60A interface, as shown in Figure C.1.a).

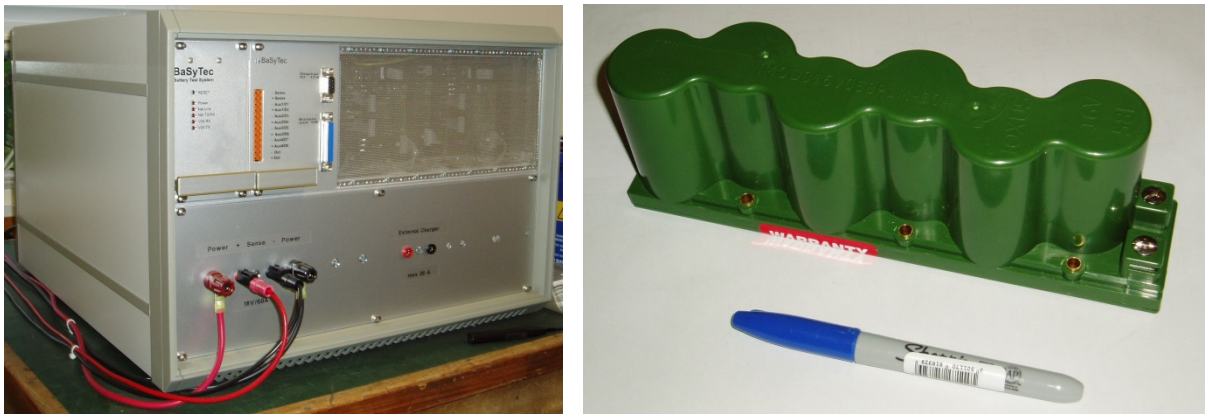


Figure C.1. a) The BaSyTec Battery test system, and
b) an Ioxus 16V / 58F supercapacitor module

The BaSyTec Battery Test System operates with a PC and integrates all requirements from design of a test plan, running battery tests, storage of results in an SQL database, and data analysis and charting tools.

The BaSyTec test system can be operated with voltage, current or power profiles, however when testing supercapacitors it must be operated in galvanostatic mode, with current set at each timestep in the test-plan.

Tests conducted include measurement of capacitance; equivalent series resistance (ESR) and response to current steps; and leakage current.

## *C.1 Capacitance measurement*

The discharge current specified by Ioxus for the capacitance test is for a 250 second discharge and is equivalent to the IEC standard Class 3 (Power) definition.

$$I_d = \frac{(4 \,.\, V_{RU} \,.\, C)}{1000}$$

where $V_{RU}$ is the rated voltage of the supercapacitor.

[17] Representative Test Procedures for Customer Evaluations. Ioxus Inc., http://www.ioxus.com
[18] http://www.maxwell.com/products/ultracapacitors/docs/applicationnote_maxwelltestprocedures.pdf
[19] IEC 62391-1 Fixed electric double-layer capacitors for use in electronic equipment - Part 1: Generic specification. International Electrotechnical Commission, 2006
[20] BaSyTec GmbH http://www.basytec.de

For the Ioxus 16V / 58F supercapacitor module, $V_{RU} = 16.2V$ and therefore the discharge current is $I_d = 3.7A$. The calculated discharge current would be the same for the individual 2.7V / 350F cells within the module. Maxwell uses a value for the discharge current of around 75 mA/F for cells, or 26.25A for a 2.7V / 350F supercapacitor cell. This is equivalent to a 36 second discharge and this faster discharge rate is claimed to be suitable for a production environment.

The module was charged at a current of 5A to a voltage of 16V, and the voltage was held within limits for 10 minutes using a small on-off cyclic charge, then discharged at $I_d = 3.7A$, see Figure C.2. The IEC 62391-1 method for calculation of capacitance was used, where $I_d$ is the discharge current, and $(t_2 - t_1)$ is the time to discharge from 80% to 40% of $V_{RU}$.

$$C = I_d \cdot \frac{(t_2 - t_1)}{(V_{80} - V_{40})}$$

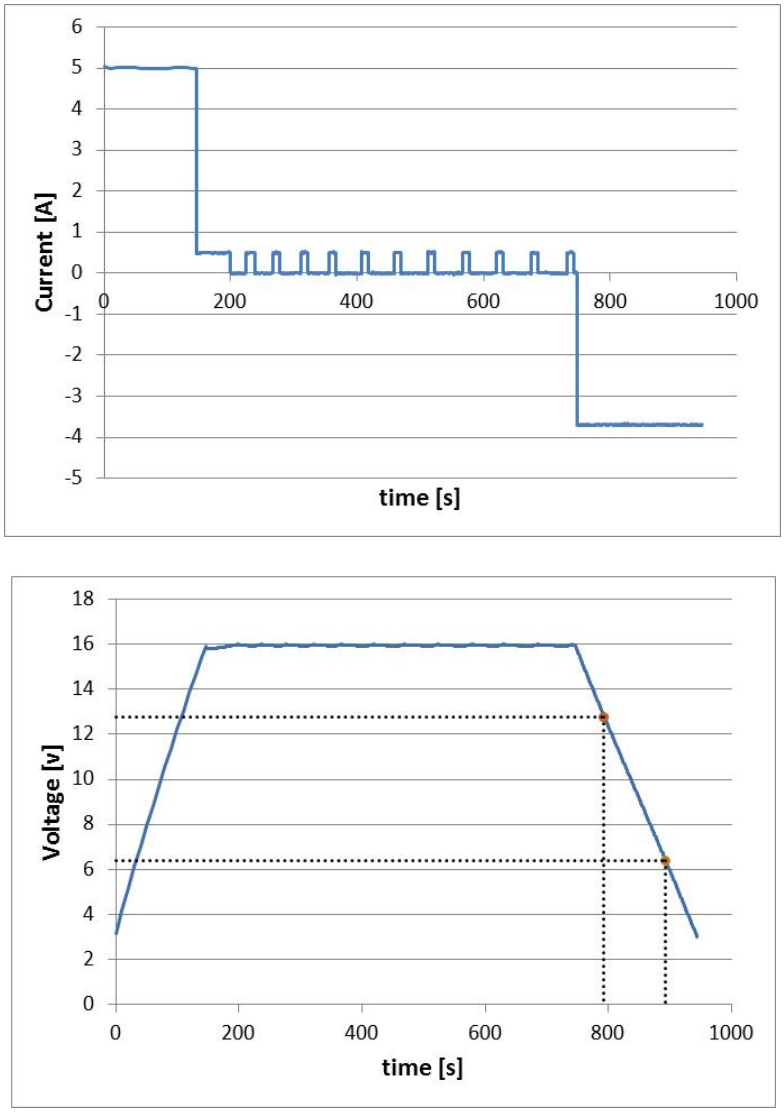


Figure C.2. Capacitance test profile: a) current, b) voltage

The hold period at the rated voltage before discharge results in a higher capacitance value as during the very slow charge rate ions can travel to the deeper pores inside the electrodes. The IEC 62391-1 test specifies a hold time of 30 minutes; Ioxus use 10 minutes; and Maxwell use 15 seconds and repeat the test to obtain a capacitance value representative of cyclic applications. In addition the voltage range over which the capacitance is measured differs substantially; IEC 62391-1 specifies 80% to 40% of rated voltage; Ioxus use 100% to a low voltage level; while Maxwell use 100% to 50%; resulting in differences between the capacitance measurements. Clearly the measurement from 100% of rated voltage will give a lower capacitance measurement, as it includes the initial voltage drop due to the ESR, which is over 0.5V for this module for a discharge current of 3.7A.

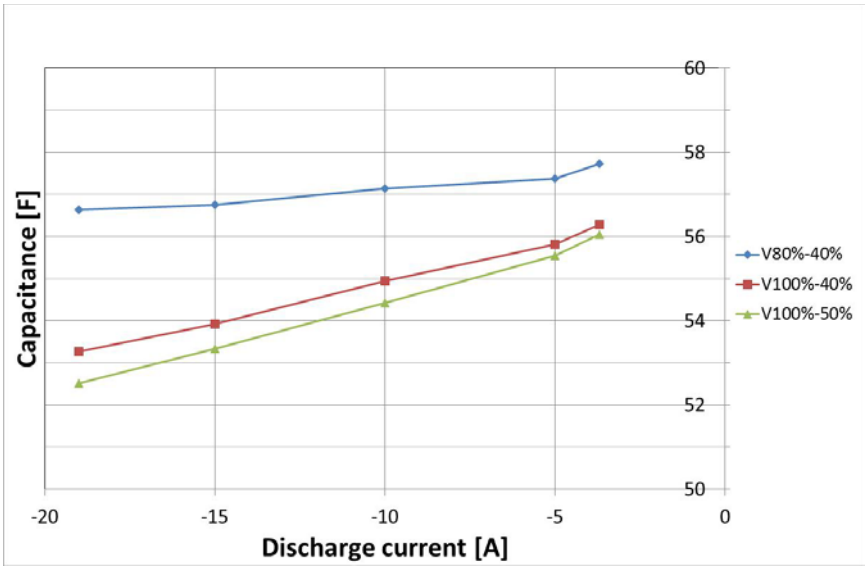


Figure C.3. Capacitance measured at various discharge currents and voltage measurement ranges

The results in Figure C.3 show that the module capacitance is close the nominal specification using the IEC Class 3 (Power) discharge current and the 80% to 40% voltage range, while the capacitance is lower at higher discharge rates. As expected, the capacitance measurement is considerably lower when the alternative voltage measurement ranges are used.

The IEC standard specifies the discharge current for Class 4 (Instantaneous Power) as ten times the Class 3 discharge current, which for the Ioxus 16V / 58F supercapacitor module would be 37A. This current is much higher than the specified maximum continuous current level of 19A, and the discharge test to 40% $V_{RU}$ would take around 15 seconds, and was not tried to avoid the risk of damaging the module. This current is twice the maximum current already tested; however it should be included in the next series of tests as it is relevant to the high current application.

## *C.2 Equivalent Series Resistance (ESR) measurement*

The IEC standard specifies measurement of the DC – ESR by first charging the supercapacitor to rated voltage, holding the voltage for a period of 30 minutes, and then applying a

discharge current step according to the classification. The test was conducted using a voltage hold time of 10 minutes and a range of discharge currents from 5A to 60A, to cover the discharge currents defined by the IEC 62191 standard, $I_d = 3.7A$ (Class 3 - Power) and $I_d = 37A$ (Class 4 – Instantaneous power). Figure C.4 shows the voltage drop following the current step and during discharge. The DC ESR is then calculated from the initial voltage drop $\Delta V$ obtained from the intersection of the linear discharge line with the discharge step time at $t_0$.

$$DC\ ESR\ = \frac{\Delta V}{I_d}$$

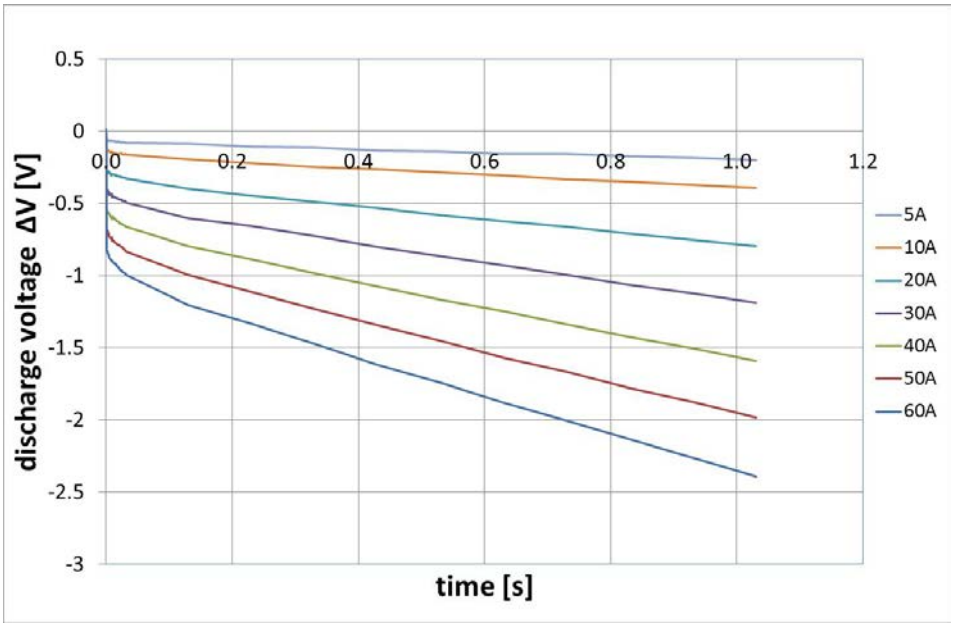


Figure C.4. Discharge voltage profile for several discharge current steps

Using the linear discharge line from 0.5 to 1.0 seconds in Figure C.4, the average DC ESR is 17.1 mΩ for the range of currents from 5 – 60A. Ioxus suggest using the linear part from 1 to 2 seconds after the discharge step, and the DC ESR specified by Ioxus is ≤23 mΩ. The slope of this part of the discharge indicates a capacitance value around 15% less than the capacitance calculated using the discharge from 80% to 40% of rated voltage, see previous section Appendix C.1.

This suggests that this part of the discharge is not linear, and to investigate further a discharge current of 20A was applied and the discharge voltage was measured for up to 3 seconds. Linear approximations for the intervals 0.5 to 1 second, 1 to 2 seconds, and 2 to 3 seconds were plotted to intersect with the start of the discharge as shown in Figure C.5.

The results for ESR and capacitance calculated using several measurement methods are shown in Table C.1, and this confirms that the single resistor – capacitor model has limitations, and for improved accuracy the parameters of an equivalent circuit with cascaded RC elements should be determined.

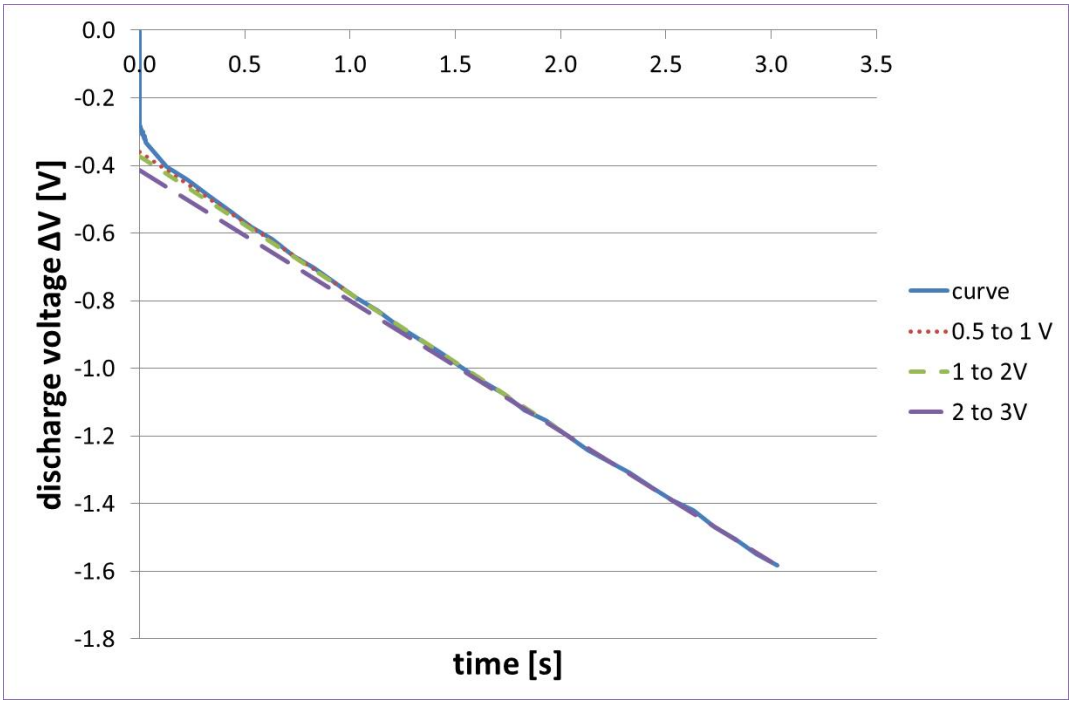


Figure C.5 Discharge curve showing linear projections

| Voltage range for linear projection [V] | DC ESR [mΩ] | Capacitance [F] |
|---|---|---|
| 0.5 to 1.0 | 18.0 | 47.9 |
| 1.0 to 2.0 | 18.7 | 49.3 |
| 2.0 to 3.0 | 20.7 | 51.7 |
| 40% to 80% $V_{RU}$ | 30.0 | 56.6 |

Table C.1. ESR and Capacitance measurements for a discharge current of 20A and using several linear projections

### *C.3 Leakage current measurement*

In the case of supercapacitor modules the current through the balancing resistors (120 Ω) is much larger than the specified leakage current for the individual cells (≤1mA after 72 hours). The specified leakage current is normally measured after 72 hours at a constant voltage and will fall during that time. The specified leakage current for the Ioxus 16V / 58F module is <25mA, which is consistent with the current through the balancing resistors. A test was conducted using a constant voltage source connected to the supercapacitor module via a 1Ω resistor, used to measure current, and after 18 hours the average current was already down to 28mA. Therefore the measured leakage current is around the expected figure.

# D. Appendix: Wind turbine rotor inertia storage

In order to analyse the stored energy in the rotor, it is necessary to have data on the rotor speed and moment of inertia. Unfortunately this data is generally not published by manufacturers; however relationships in the form of trends for rotor mass and inertia can be derived, based on basic relationships and empirical fits to available data for turbine power and rotor diameter.

The relationships describe the trends much more accurately than simply using the so-called square-cube law, where power is proportional to the square of the rotor diameter, and blade mass is proportional to diameter cubed.

The most detailed data available is for the NREL 5-MW wind turbine, and this has been used as a reference for the trendlines.

## *D.1 NREL 5MW reference turbine*

The NREL 5MW reference wind turbine for offshore development was derived from publicly available information on the Multibrid M5000 and Repower 5M prototype wind turbines, and used properties from several conceptual models. The composite result was claimed in 2009 to use the best available and representative specifications. The key parameters are given in Table D.1.

| | |
|---|---|
| Rotor diameter | 126m |
| Hub diameter | 3m |
| Rotor mass | 110 tonne |
| Blade length | 61.5m (w.r.t. blade root) |
| Blade mass | 17.74 tonne |
| Blade moment of inertia | 11,776,047 kg.m$^2$ (w.r.t. blade root) |
| Blade Centre of Mass (CM) location | 20.475m (w.r.t. blade root) |

Table D.1. NREL 5MW turbine parameters [ref. Tables 1-1 & 2-2 in Jonkman (2009)]

The Parallel Axis Theorem states that if the axis of rotation is displaced a perpendicular distance r from the Centre of Mass, then the moment of inertia $I_r$ about the displaced axis is given by the expression:

$$I_r = I_{CM} + m\ r^2$$

where $I_{CM}$ is the moment of inertia about the Centre of Mass and m is the mass.

The moment of inertia about a parallel axis can be calculated from the moment of inertia for any axis. For two parallel axes, with perpendicular distances $r_1$ and $r_2$ from the centre of mass, the corresponding moments of inertia $I_{r1}$ and $I_{r2}$ are given by:

$$I_{r1} = I_{CM} + m\ r_1{}^2$$

and

$$I_{r2} = I_{CM} + m\ r_2{}^2$$

and therefore

$$I_{r2} = I_{r1} + m\ (r_2{}^2 - r_1{}^2)$$

For the NREL 5MW rotor, $r_1$= 20.475m and for the 3m diameter hub, $r_2$ = 20.475 + 1.5 m; the moment of inertia of each blade about the rotor (hub) axis is 12,905,642 kg.m$^2$; and the moment of inertia of the 3 blades is 38,716,925 kg.m$^2$.

The moment of inertia of a thin walled cylinder of mass m and radius r is $I = m\ r^2$. The hub mass is 56,780 kg and the radius is 1.5m, and assuming the hub is a thin walled cylinder then its moment of inertia is 127,755 kg.m2, much less ( < 0.3% ) than the moment of inertia of the blades. The actual inertia of the hub, with actual mass distribution, will be less than this value; however this will not introduce a significant error for the overall rotor.

Therefore the total moment of inertia of the NREL 5MW rotor is 38,844,680 kg.m$^2$.

## *D.2 Power and Rotor diameter*

The power in the wind is proportional to the swept area, and the relationship between wind turbine rated power and rotor diameter can be expected to be in the form:

$$RatedPower = k_1 \cdot RotorDiameter^{k_2}$$

As the rotor increases in diameter the wind turbine also increases in height, and wind speed increases with height due to wind shear. Therefore the rated power may be expected to increase more than in proportion to the swept area, and the exponent $k_2$ may be greater than 2. EWEA Facts (2004) observes that using typical parameters for the wind shear effect for land-based sites, the rated power can be expected to vary as $(RotorDiameter)^{2.4}$. However large wind turbines are primarily designed for deployment offshore where the wind shear effect is reduced and the relationship may be expected to be different to wind turbines designed for land-based sites. EWEA Facts (2004) Table 1.2 shows the progression of the exponent in the relationship over time (and with increasing rotor diameter), showing the exponent reducing from 2.320 in 1996, to 2.075 in 2003. As shown in Figure D.1, using parameters $k_1 = 0.00022$ and $k_2 = 2.073$ in the relationship (where rated power is in MW and rotor diameter is in metres), provided a satisfactory fit to the data for 35 wind turbines in 2004.

$$RatedPower = 0.00022 \cdot RotorDiameter^{2.073}$$

Using more recent data the trendline still provides a reasonable fit as shown in Figure D.1 (including data from Wind Energy The Facts EWEA 2009 Table 1.3.9), and Figure D.2 (including data for 2014 turbines). In particular the NREL 5-MW reference turbine is on the trendline so there is no need to adjust the coefficients. The data includes Enercon and Vestas turbines designed for several wind classes, where turbines designed for lower wind speed regimes, or with lower tower height, have larger diameter rotors for the same rated power, resulting in a spread on the graph.

The rotor diameter of the Enercon rotor is smaller than the trend for a given power, possibly because it is designed for high wind onshore sites and is mounted on a very high tower, with hub height 135m. Specifications for the 8MW Vestas V164-8 and the 6MW Siemens SWT-6-154 quote the tower height as site-specific, although Vestas has stated a typical hub height of about 107m.

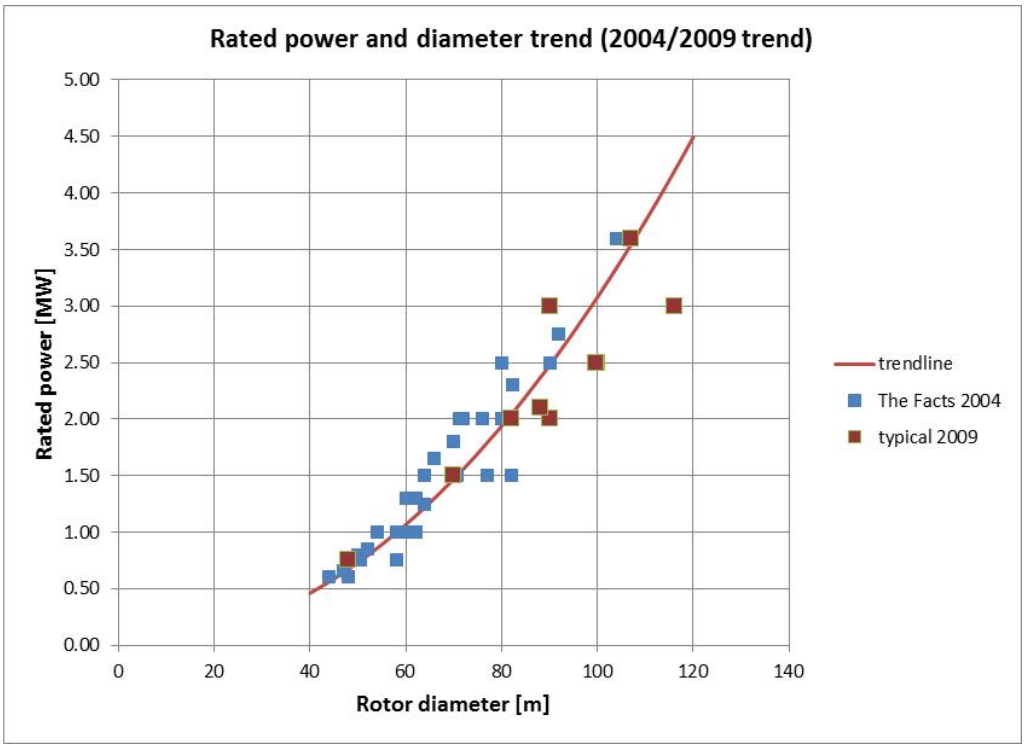


Figure D.1. Rated power and diameter data (2004 & 2009 data), and trendline

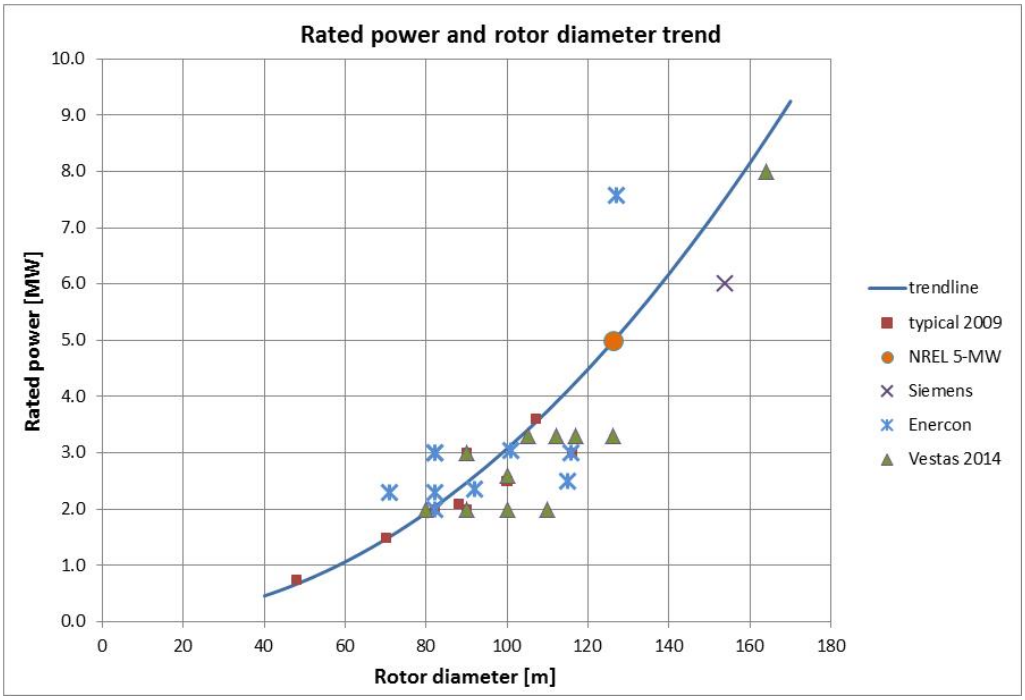


Figure D.2. Rated power and diameter data (2014), and trendline

## *D.3 Rotor Speed and Diameter*

The main reason to increase tip speed with rotor diameter is that rotor torque is reduced, resulting in nacelle mass and cost reduction. Although noise increases with tip speed this is less of a problem in large wind turbines that tend to be installed offshore, as discussed in Wind Energy - The Facts (2009). Data for wind turbines in 2004 showed an increasing trend and data for 2009 also fits this trend. The trendline shown in Fig 1.3.21 of Wind Energy – The Facts (2009) and formalised by de Haan (2011) is:

$$TipSpeed\ [m/s] = \ 0.5714\ .radius\ [m]\ +\ 50$$

As shown in Figure D.3 there is a clear trend of increasing tip speed with turbine size, although there is a wide spread of data. Very large wind turbines tend to use high tip speeds to restrict nacelle mass, as discussed in Wind Energy - The Facts (2009), while the ceiling is likely to be around 90 m/s. This suggests that there may be much less spread for very large turbines, and Figure D.4 appears to show this. The data shown in Figure D.4 is for the NREL 5-MW reference turbine, the 6MW Siemens SWT-6-154, and the Vestas V164-8 8MW and V90-3.0 3MW, where data was available for nominal rotor speed.
The trendline coefficients have been adjusted to fit available data for large wind turbines, and in particular the NREL 5-MW reference turbine, resulting in the modified relationship:

$$TipSpeed\ [m/s] = \ 0.482\ .radius\ [m]\ +\ 50$$

Although the trend has been presented in terms of the blade tip speed, the rotor speed is required to determine rotor kinetic energy:

The standard equations for tip speed and rotor rotational speed are

$$TipSpeed\ [m/s] = radius[m]\ \cdot\ RotorSpeed\ [rad/s]$$

$$Rotor\ speed\ [rad/s] = \ tip\ speed\ [m/s]\ /\ radius\ \ [m]$$


Figure D.3. Blade tip speed trend using 2004 & 2009 data

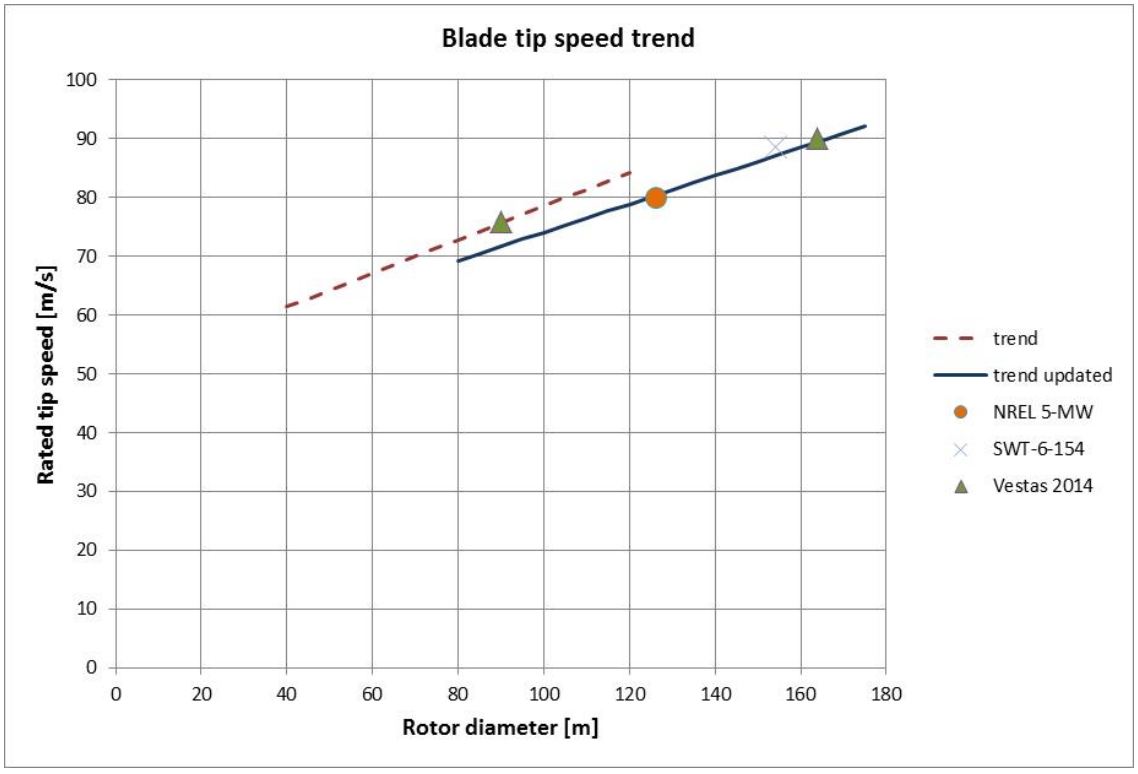


Figure D.4. Blade tip speed trend modified for large wind turbines

## *D.4 Rotor mass*

Rotor mass is generally not published by wind turbine manufacturers. Blade mass and nacelle mass are sometimes quoted, presumably because these are of interest when assessing the feasibility and cost of transportation and erection. In the case of the Vestas V164, the mass of each blade is specified as 35 tonne, and the rotor mass is 210 tonne, see Vries (2011), twice the total mass of the blades. In the case of the NREL 5-MW turbine, where the rotor mass is 110 tonne, and the blades are 17.74 t, the ratio $total\ rotor\ mass\ /total\ blade\ mass$ is 2.07. A typical 2MW wind turbine described by Schubel (2012) has a rotor weight 36 t, with blade mass 5.80 t, and also gives a ratio of 2.07. This factor may be used to estimate the rotor mass where only the blade mass is specified.

A trendline first proposed to fit 2004 wind turbine data, Wind Energy – The Facts (2004), Fig 1.15, is shown in Figure D.5 as "trend 2004". The trendline parameters have been modified to fit the NREL 5MW reference turbine, and the updated trendline for large wind turbines, showing a further reduction from a cubic scaling, is proposed as:

$$RotorMass = 0.000486 \cdot RotorDiameter^{2.55}$$

where rotor mass is in tonne, and rotor diameter is in metres

This trendline is a good fit to the Vestas V164-8 turbine parameters, and is also a reasonable fit to rotor mass and diameter parameters for Vestas wind turbines, described by de Haan (2011).

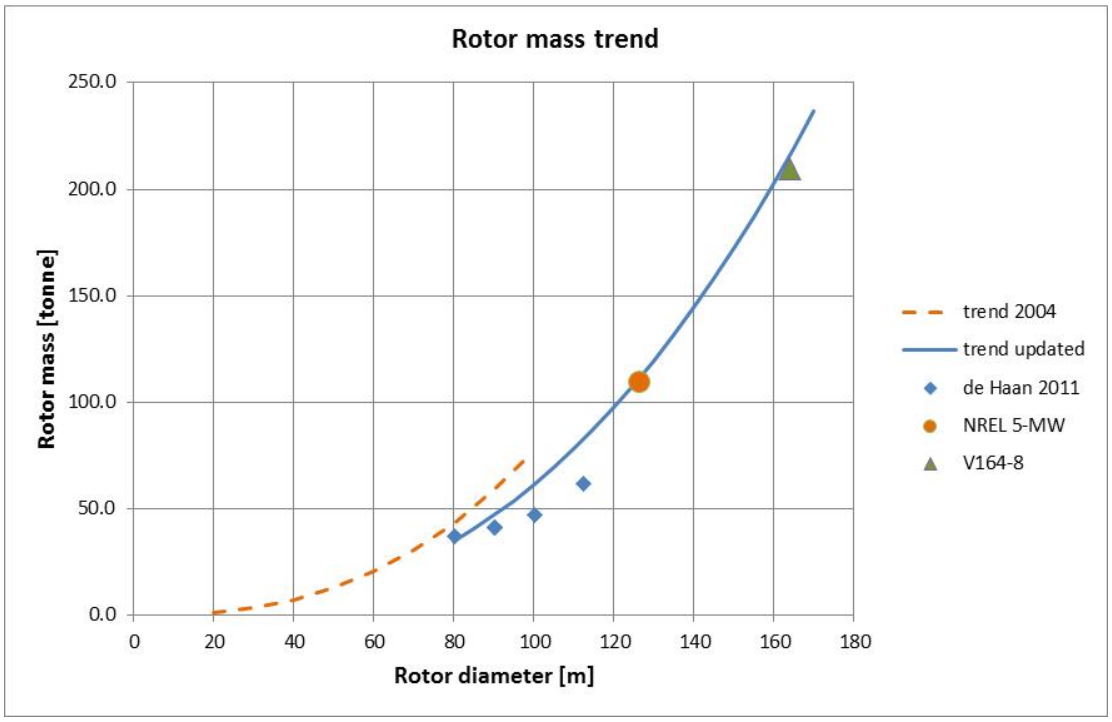


Figure D.5. Rotor mass vs. rotor diameter trend

The blade mass scaling relationships for several designs are graphically illustrated in a report by Fingersh (2006), Figure 1, showing the large reductions in blade mass achieved by that date. The advanced mass scaling relationship in the report, $BladeMass\ [kg] = 0.4948 \cdot RotorRadius^{2.53}$, produces a blade mass that when multiplied by 3 blades and by 2.07 to include the hub mass, produces a rotor mass that very closely matches the rotor mass – diameter relationship above.

Equations for power as a function of diameter, and mass as a function of diameter can be combined to give the rotor mass – power trend, as shown in Figure D.6.

$$RotorMass = 0.000639 \cdot Power^{1.23}$$

where Rotor Mass is in kg and Power is in watts.

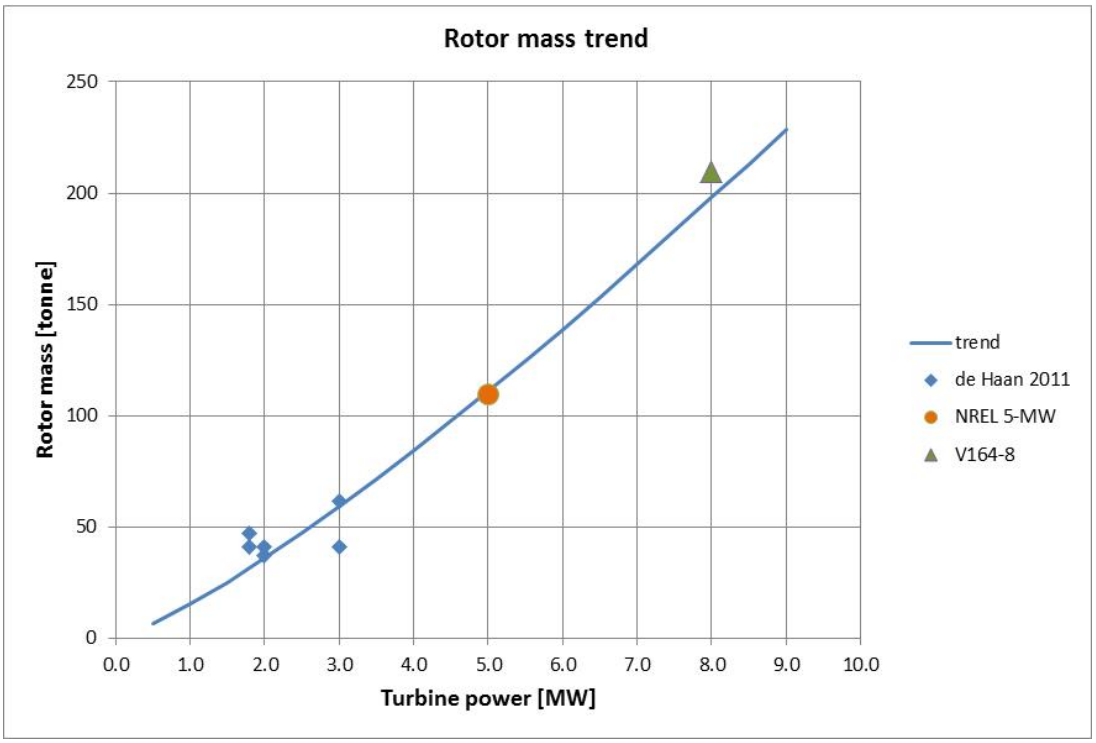


Figure D.6. Rotor mass vs. turbine power trend

Using the mass-power relationship, the Siemens SWT-6-154 6MW turbine with 154m diameter rotor is estimated to have a mass of 139 tonne, while using the mass-diameter relationship, the mass is estimated to be 184 tonne.

Efforts by manufacturers are successfully reducing blade mass (and cost), and rotor mass, and the mass-diameter trendline may over-estimate the rotor mass. For example, Gamesa reported a weight reduction of 25% in the Gamesa G128-4.5MW turbine[21], where the rotor diameter is 128m, and the approximate blade mass is 15 t and the rotor mass is estimated as 90 t. In this case the mass-power trendline provides the best estimate for the mass (97 t), while the mass-diameter trendline overestimates the rotor mass (115 t). The offshore

[21] http://www.gamesacorp.com/en/products-and-services/wind-turbines/

variant Gamesa G128-5MW, with increased power, uses the same rotor and in this case the mass-power trend estimates the rotor mass as 111 tonne; this is still a better estimate than obtained using the mass-diameter trend.

In the case of the Vestas V164-8.0 wind turbine[22], the mass estimates are 198 tonne (using the mass-power relationship) and 216 tonne (using the mass-diameter relationship), while the actual rotor mass [23] is 210 tonne.

Tower height for the both the Siemens and Vestas turbines is specified as "site specific", although Vestas is reported to have stated a typical hub height of about 107m. Gamesa specifies a tower height of 80-94m and site-specific for the offshore 5MW turbine, and specifies tower heights of 81, 95, 120, 140 m for Gamesa onshore 4.5MW and 5.0 MW turbines, using the same diameter rotor. The fact that appropriate tower heights are used in different wind regimes generally explains why the trends apply to both offshore and onshore turbines.

This is summarised in Table D.2:

| Turbine | Power [MW] | Diameter [m] | Rotor mass [tonne] | | |
|---|---|---|---|---|---|
| | | | Actual (using 2x blade mass) | mass-power estimate | mass-diameter estimate |
| Siemens SWT-6-154 (Offshore) | 6 | 154 | no data | 139 | 184 |
| Vestas V164-8.0 (Offshore) | 8 | 164 | 210 | 198 | 216 |
| Gamesa G128-4.5MW (Onshore) | 4.5 | 128 | 90 | 97 | 115 |
| Gamesa G128-5MW (Offshore) | 5 | 128 | 90 | 111 | 115 |

Table D.2. Rotor mass for large wind turbines

In conclusion, it is clear that the mass estimates are approximate for different wind turbines, as the mass depends on the blade structure and materials, and also depends on the intended wind regime. Based on limited available rotor mass data, it appears that the mass-diameter relationship over-estimates rotor mass. Therefore where mass is not specified by the manufacturer, it is recommended that the mass-power relationship is used, to avoid overestimating rotor mass and related parameters such as the inertia constant.

[22] http://www.mhivestasoffshore.com/innovations/
[23] WindPower Monthly 14-April 2011. http://www.windpowermonthly.com/article/1065676/close---vestas-v164-7mw-offshore-turbine

### *D.5 Rotor inertia constant*

An expression for the blade and rotor moment of inertia may be expected to be of the form:

$$I_r = k \cdot m \cdot r^2$$

A thin rod of length r and mass m uniformly distributed along its length has $k = 1/3$. Clearly a wind turbine blade has a non-uniform mass distribution, with much more mass near the root, and therefore a value of $k$ much smaller than 1/3 is to be expected. There are a few discussions about blade moment of inertia in the literature. De Haan (2011) presented a relationship for wind turbine (rotor) inertia, although without analytical justification, suggesting that $k = 1/9$ , while Rodriguez (2007) analysed a 26m blade with an assumed mass distribution and obtained $k = 0.212$ , and also referred to other estimates for 20m and 62m blades, where $k = 0.222,\ 0.197$ respectively.

Numerical analysis of rotor inertia requires detailed information about the blade and hub mass distribution, and in principle this analysis is straightforward. Alternatively the moment of inertia could be measured using methods described by Gracey (1948) and Jardin (2010), in practice this would present a challenge for large blades. Inertia data published for the NREL 5MW reference turbine[24] was calculated numerically by the FAST software (as described in the NREL Technical report) and based on the known distribution of blade mass and hub mass and inertia. Using the NREL 5MW specification for rotor mass, diameter and moment of inertia, we find that using the constant $k = 0.089$ in the expression above gives a good fit.

Therefore we use the expression for the Rotor moment of inertia:

$$RotorMomentOfInertia = 0.089 \cdot RotorMass \cdot RotorRadius^2$$

And by definition, the rotor kinetic energy is given by:

$$RotorKineticEnergy = \frac{1}{2} \cdot RotorMomentOfInertia \cdot RotorSpeed^2$$

The inertia constant is defined as $H = E/S$ where E is the kinetic energy of the rotating mass and S is the rated power, and is equivalent to the storage time in seconds. Rotor kinetic energy and turbine power increase rapidly with rotor diameter; however the ratio is nearly linear, as shown in Figure D.7.

The specified data for rotor speed, rotor mass, and moment of inertia for the NREL 5MW turbine has been used to provide a reference point for the trendlines shown in Figures D.7, D.8 and D.9. In the case of the Vestas V164-8 turbine, rotor speed and rotor mass data are available, and were used in the calculation of inertia constant. In the case of other current Vestas turbines (labelled in the Figures as Vestas 2014), the Siemens turbine and the Enercon turbines, only rated power and rotor diameter are specified on the respective

[24] NREL Technical Report NREL/TP-500-38060. February 2009. Available online from: http://www.osti.gov/scitech/biblio/947422

manufacturer's website, and the rotor speed-diameter and mass - power relationships in the earlier sections were used.

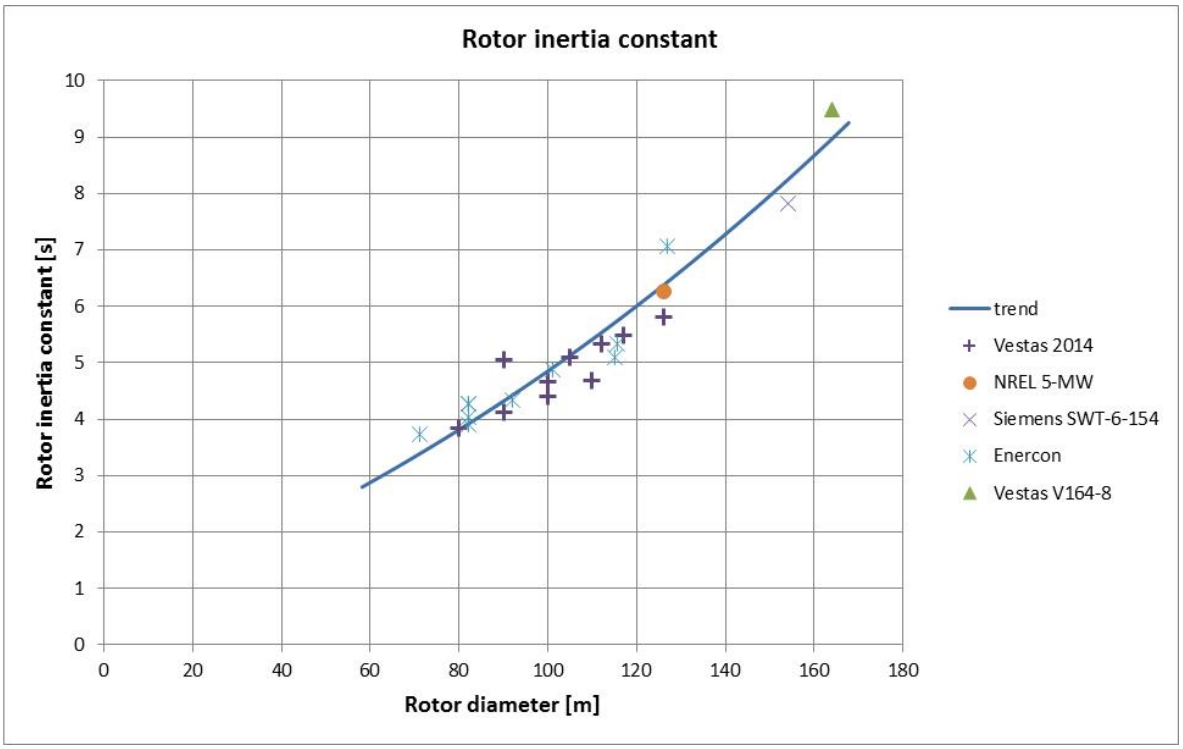


Figure D.7. Rotor inertia constant vs. Rotor diameter

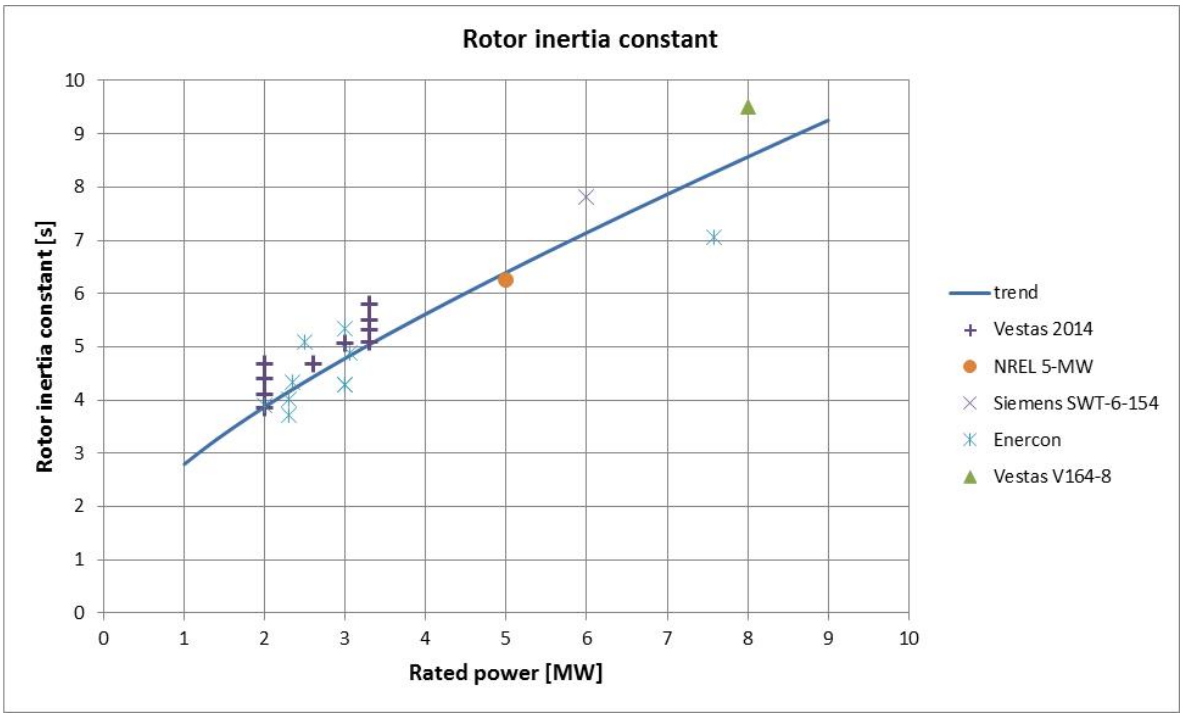


Figure D.8. Rotor inertia constant vs. Rated power

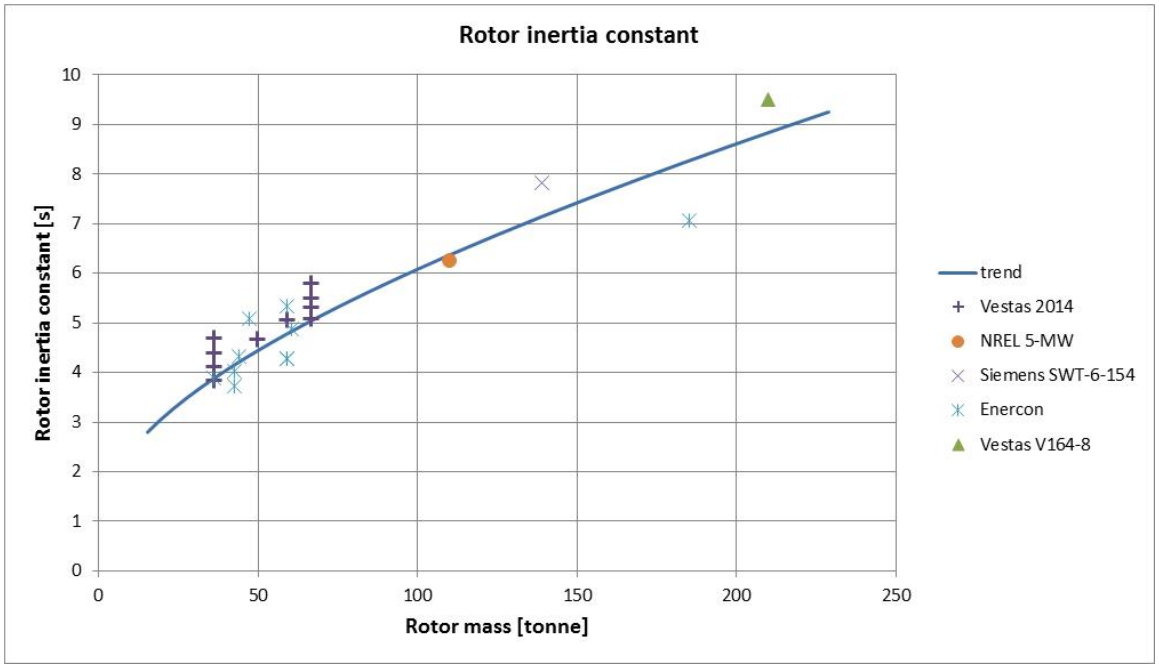


Figure D.9. Rotor inertia constant vs. Rotor mass

As noted in Table D.2, in the case of the Vestas V164-8.0 wind turbine, the mass estimates are 198 tonne (using the mass-power relationship) and 216 tonne (using the mass-diameter relationship), while the actual rotor mass is 210 tonne. The corresponding inertia constant estimates are 8.98s, 9.76s, and 9.49s. Therefore where mass is not specified, using the mass-power relationship avoids over-estimating the rotor mass and inertia constant.

In conclusion, the total inertia constant can be up to around 10 seconds for large wind turbines. The rotor inertia can be used in a variable speed wind turbine to reduce torque transients, optimise energy capture, and smooth power output. However only a fraction of the total rotor inertia could be available as 'on demand' storage, and depending on the application for storage, either to absorb energy (LVRT and high frequency response) or produce energy (primary and secondary frequency response), the rotor may be operated below or above the optimum speed, resulting in loss of energy production.

### *D.6 Inertia constant of a large wind turbine*

The Siemens SWT-6-154 wind turbine was chosen for inclusion in simulation studies. The manufacturer's website[25] specifies rated power, rotor diameter and rotor speed range. Estimates for rotor mass, blade tip speed, and rotor moment of inertia have been obtained from trendlines derived from wind turbine data, and referenced to the detailed specifications of the NREL 5MW wind turbine. This is summarised in Table D.3.

| **Specified:** | |
|---|---|
| Rated power | 6 MW |
| Rotor diameter | 154 m |
| Rotor speed range | 5 – 11 rev/min (0.53 – 1.15 rad/s) |
| **Derived:** | |
| Rotor mass | 139.01 t (using the mass-power relationship) |
| Nominal rotor speed | 1.13 rad/s |
| Rotor moment of inertia | 73,351,000 kg.m$^2$ |
| Rotor kinetic energy | 46,943,000 J |
| Inertia time constant | 7.82 s |

Table D.3. Specified and derived parameters for the Siemens SWT-6-154 wind turbine

The trendlines used for derived parameters are described in earlier sections, and are summarised here:

Rated power [W] and rotor mass [kg] as a function of rotor diameter [m]:

$$RatedPower = 220 \cdot RotorDiameter^{2.073}$$
$$RotorMass = 0.486 \cdot RotorDiameter^{2.55}$$

These can be combined to give rotor mass [kg] as a function of rated power [W]:

$$RotorMass = 0.0006386 \cdot RatedPower^{1.2301}$$

The nominal tip speed [m.s$^{-1}$] and rotor angular speed [rad.s$^{-1}$] are:

$$BladeTipSpeed = 0.482 \cdot RotorRadius + 50$$
$$RotorAngularSpeed = BladeTipSpeed \; / \; RotorRadius$$

The rotor moment of inertia [kg.m$^2$] is:

$$RotorMomentOfInertia = 0.089 \cdot RotorMass \cdot RotorRadius^2$$

And by definition the rotor kinetic energy [kg.m$^2$] and inertia time constant [s] are:

[25] http://www.energy.siemens.com/br/pool/hq/power-generation/renewables/wind-power/6_MW_Brochure_Jan.2012.pdf

$$RotorKineticEnergy = \frac{1}{2} \cdot RotorMomentOfInertia \cdot RotorAngularSpeed^2$$

$$InertiaTimeConstant = \frac{RotorKineticEnergy}{TurbineRatedPower}$$

## *D.7 References to Appendix D*


de Haan J.E.S., Frunt J., Kling W.L., Wind Turbines Kinetic Energy Storage Potential for Frequency Support, *Proc. EWEA 2011 Conference*, Brussels, 14-17 March 2011

EWEA (2004). *Wind Energy - The Facts 2004 – an analysis of wind energy in the EU-25, Volume 1 - Technology*. EWEA, Feb 2004. [Available from: http://www.ewea.org/fileadmin/ewea_documents/documents/publications/WETF/Facts_Volume_1.pdf ]

EWEA (2009). *Wind Energy – The Facts 2009, Part I: Technology*, A consortium project led by EWEA and funded by Intelligent Energy Europe, March 2009.
[Available from: http://www.wind-energy-the-facts.org/ ]

Fingersh L., Hand M., Laxson A., (2006) Wind turbine design cost and scaling model, *NREL Technical Report NREL/TP-500-40566*, December 2006.
[Available from: https://www.osti.gov/scitech/biblio/897434-wind-turbine-design-cost-scaling-model)

Gracey W., (1948) The experimental determination of the moments of inertia of airplanes by a simplified compound-pendulum method, *National Advisory Committee for Aeronautics (NACA) Technical Note No. 1629*, Washington, June 1948.
[Available from: http://naca.central.cranfield.ac.uk/reports/1948/naca-tn-1629.pdf ]

Jardin M, (2010) Improving Mass Moment of Inertia Measurements, *The Mathworks*, Technical Article, 2010.
[Available from: http://www.mathworks.co.uk/company/newsletters/articles/improving-mass-moment-of-inertia-measurements.html ]

Jonkman J., Butterfield S., Musial W., Scott G., (2009) Definition of a 5-MW Reference Wind turbine for Offshore System Development, *NREL Technical Report NREL/TP-500-38060*. February 2009. [Available online from: http://www.osti.gov/scitech/biblio/947422 ]

Rodríguez, ÁG González, A. González Rodríguez, and M. Burgos Payán. (2007) Estimating wind turbines mechanical constants. *Proc. Int. Conf. Renewable Energies and Power Quality (ICREPQ'07)*, pp. 27-30. 2007.

Schubel P.J., Crossley R.J., (2012) Wind Turbine Blade Design, *Energies 2012*, 5, pp. 3425-3449 5(9), 3425-3449; doi:10.3390/en5093425
[Available from: http://www.mdpi.com/1996-1073/5/9/3425 ]

Vries E., Close up - the Vestas V164 7MW offshore turbine, Windpower Monthly 14-April-2011
Available from: http://www.windpowermonthly.com/article/1065676/close---vestas-v164-7mw-offshore-turbine